NUCLEAR MAGNETIC RESONANCE LINEWIDTH STUDIES OF MODEL MEMBRANES

Thesis by

Charles H. Seiter

In Partial Fulfillment of the Requirements
For the Degree of
Doctor of Philosophy

California Institute of Technology
Pasadena, California 91109

1974

(Submitted January 7, 1974)

Tóth Loretta számára. Ő nagyon okos tanárnő.

ACKNOWLEDGMENTS

Following group tradition, I would first like to thank Mrs. Karen Gleason for her expert manuscript preparation in this and other instances.

I would like to thank Dr. Gerald Feigenson for seven or eight hundred interesting discussions and his participation in equally numerous good times.

Dr. Sunney Chan has been very patient during the slower passages of this work, and also deserves thanks from me for his constant emphasis on communications problems and on the broader biological context of chemical physics.

I would also like to acknowledge many scientific discussions with Mr. William R. Furman.

Finally, I would like to thank Dr. R. W. Vaughan for much information on newer methods in magnetic resonance and for his valuable help with part of this work. I also acknowledge several experimental and philosophic conversations with Mr. Dennis Toth and Mr. Robert Fisher, and commend as well the Chan group in general as an educational organization.

ABSTRACT

The possible applications of magnetic resonance spectroscopy to current problems in membrane biophysics are surveyed with a particular view to the use of newer Fourier transform and multipulse techniques. Two contributions to this field are presented. The first contribution describes a Fourier transform filtering technique which removes the broad proton magnetic resonance (pmr) lines characteristic of cell membranes and unsonicated lipid bilayers to allow observation of methyl proton and other sharp resonance peaks. The interaction of valinomycin with lipid bilayers is monitored by this method, and the valinomycin is found to interact primarily with the polar choline head groups of the lecithin molecules in the bilayer. The second contribution analyzes the pmr linewidths of sonicated and unsonicated bilayers by the stochastic linewidth method of P. W. Anderson. It is found that the local packing of lipid chains in sonicated vesicles is significantly less orderly than the local packing in unsonicated bilayers. It is also shown that the sharp methyl resonances observed in pmr spectra of unsonicated bilayers correspond to the central spike characteristic of the methyl rotor dipolar powder spectrum in solids, and that this powder spectrum is only partially averaged by the restricted molecular motions available to lipids in unsonicated bilayers. Finally, a Waugh multipulse spectrum of unsonicated bilayers is used to establish kink formation on a timescale of 10^{-7}

sec as the chief mode of local molecular motion for protons on lipid hydrocarbon chains in unsonicated systems, as compared to trans-gauche bond rotations on a timescale of 5×10^{-9} sec or faster as the mode of local motion of protons in sonicated vesicles. The value of these two systems as model membranes is discussed in the light of these motional results.

TABLE OF CONTENTS

PART I

Introduction

The recent history of membrane biology illustrates clearly the interplay between conceptual models of biological systems and the experimental approaches these models suggest. The main purpose of this introduction is to explain the context in which the two following manuscripts should be viewed, that is, to emphasize the way physical chemistry experiments can induce changes in the conceptual models used to explain biological reality, so that new models emerge from this process and in turn suggest new experiments, with this cycle recurring until the phenomena in question are considered to be "well understood". Most researchers in the field of biomembranes would probably agree that this endpoint is nowhere in sight yet in their field. After a brief survey of the evolution of current membrane models, this section will examine the value of magnetic resonance spectroscopy as an approach to the physical solution of some membrane problems, and indicate how the contributions of Part II figure in this approach.

Evolution of General Membrane Models

Gorter and Grendel,[1] in the late 1920's, extracted the lipids from a sample of red blood cells and spread these lipids in a monomolecular layer on a Langmuir trough. Assuming that this

layer was structurally similar to monolayers of soap (i.e., hydrophilic head in the water, hydrophobic chains in the air), they estimated that the red blood cell lipids were sufficient to cover the surface of the cells twice. Reasoning from this experiment and studies of the effect of proteins on the surface tension of lipid-water interfaces,[2] Danielli and Davson offered the famous membrane model shown schematically in Fig. 1.[3] The cell is presumed surrounded by a lipid bilayer membrane coated on both sides with protein.

Early X-ray investigations[4, 5] inspired by this model confirmed that myelin at least has the general features of the Davson-Danielli model, and more recent work has shown that the membranes of red blood cells,[6] mitochondria,[7] and mycoplasma laidlawii[8] all show the same type of trilaminar structure predicted by the model. The spacing of the layers was in general agreement with that which would be expected for protein layers separated by lipid bilayers, varying from ~ 50-100 Å depending on the particular membrane chosen. Electron microscopy studies,[9] however, have suggested a modification of this structure, as shown in Fig. 2. The trilaminar structure confirmed by X-ray studies also appeared in this electron microscopy work, but the differential staining of the two sides of the membrane suggested the so-called unit membrane structure, in which one side of the lipid bilayer is covered with mucoprotein or mucopolysaccharide, and the other side with extended polypeptide chains. Thus, what might be considered the

FIGURE 1

The original Davson-Danielli cell membrane model. Globular protein covers the outside of a continuous lipid bilayer.

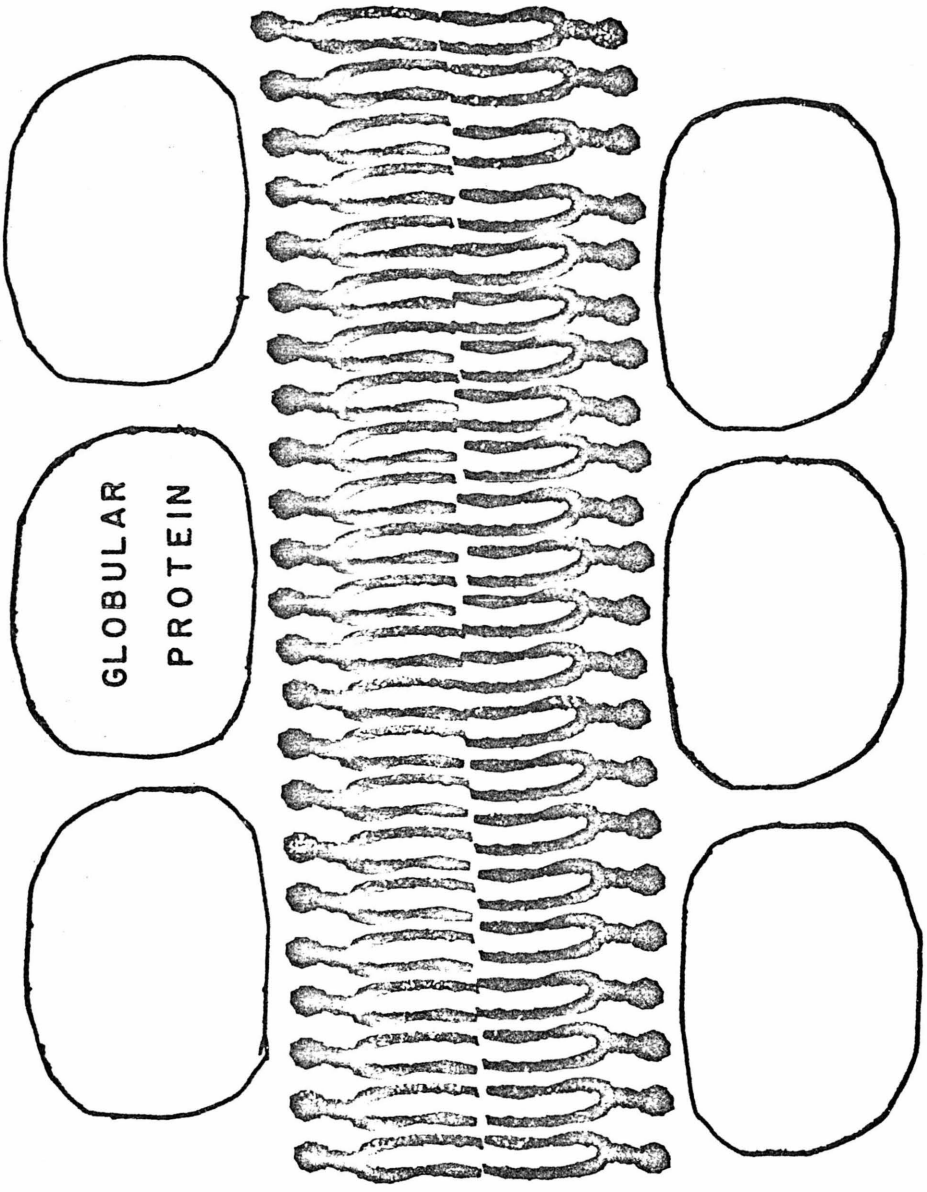
GLOBULAR
PROTEIN

FIGURE 2

Robertson's "unit membrane" modification of the Davson-Danielli model. In this model the protein chains are at least partly unfolded, and the distribution of non-lipid components favors mucoprotein or mucopolysaccharides on the cell surface.

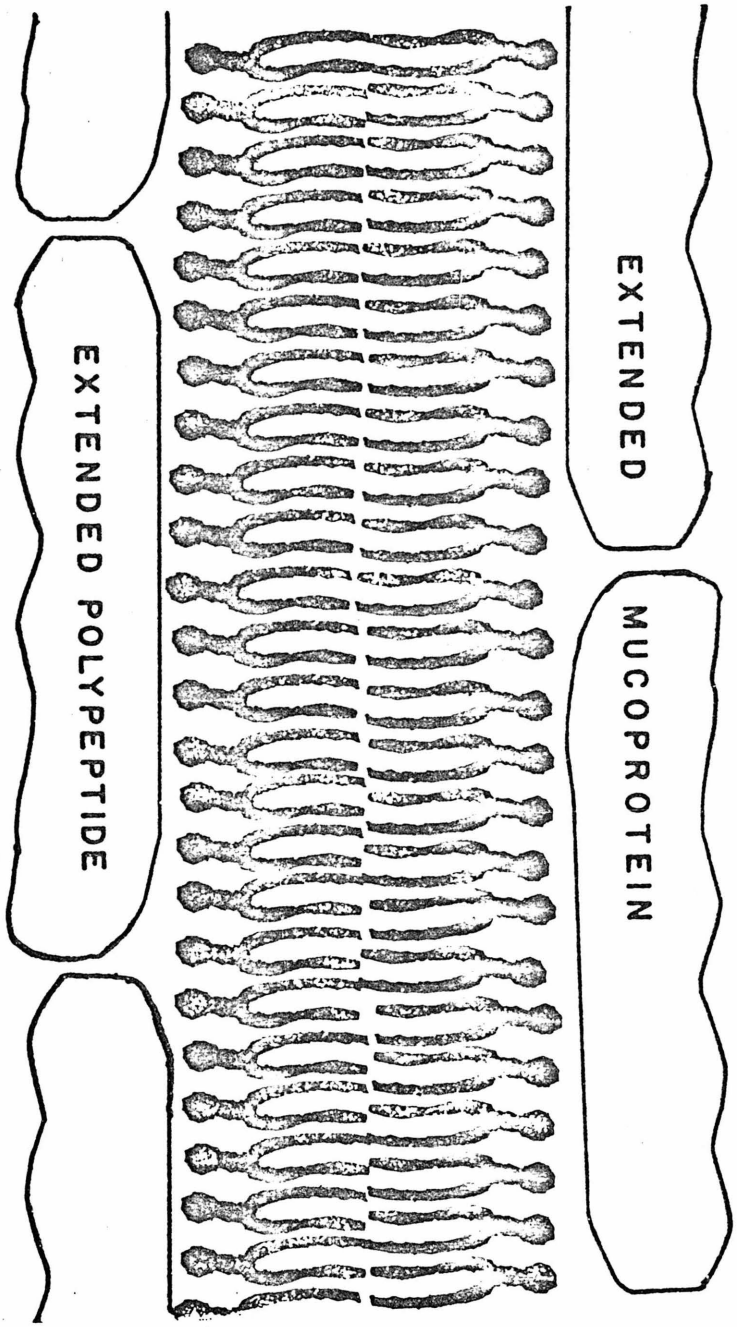
EXTENDED
MUCOPROTEIN
EXTENDED POLYPEPTIDE

first round of modifications of the original hypothesis of Gorter and Grendel has resulted in the formation of two models, the Davson-Danielli and unit membrane models. The presence of lipid bilayers in real cell membranes may be considered established, and these models focus attention on the organization of protein components of the membrane, a considerable advance in molecular structural resolution.

Further electron microscopy[10] and enzymatic modification[11] has suggested that proteins penetrate the lipid bilayer, and that these protein inlays are responsible for the characteristic behavior of membranes. An extreme form of this suggestion is that the membrane itself is an aggregation of lipo-protein units.[12] The minimum form of this hypothesis would be that the behavior of lipid-plus-protein systems more nearly imitates some aspects of the behavior of lipid bilayers than does the lipid bilayer alone. This minimum assertion is well supported by studies of ion conductance[13] across bilayers, in which it has been found that the addition of macrocyclic polypeptides such as valinomycin and gramicidin to bilayers[14] confer on the system fairly realistic transport properties such as ion selectivity. Thus another membrane model, Fig. 3, could be considered to have been generated by these physical studies.

It is clear, however, that the location of protein in the lipid matrix will depend on the nature of the membrane being studied. While questions about protein organization at the simplest

FIGURE 3

Further modification of the original membrane model by Stoeckenius. This model incorporates electron microscope evidence for protein penetration of the lipid bilayer.

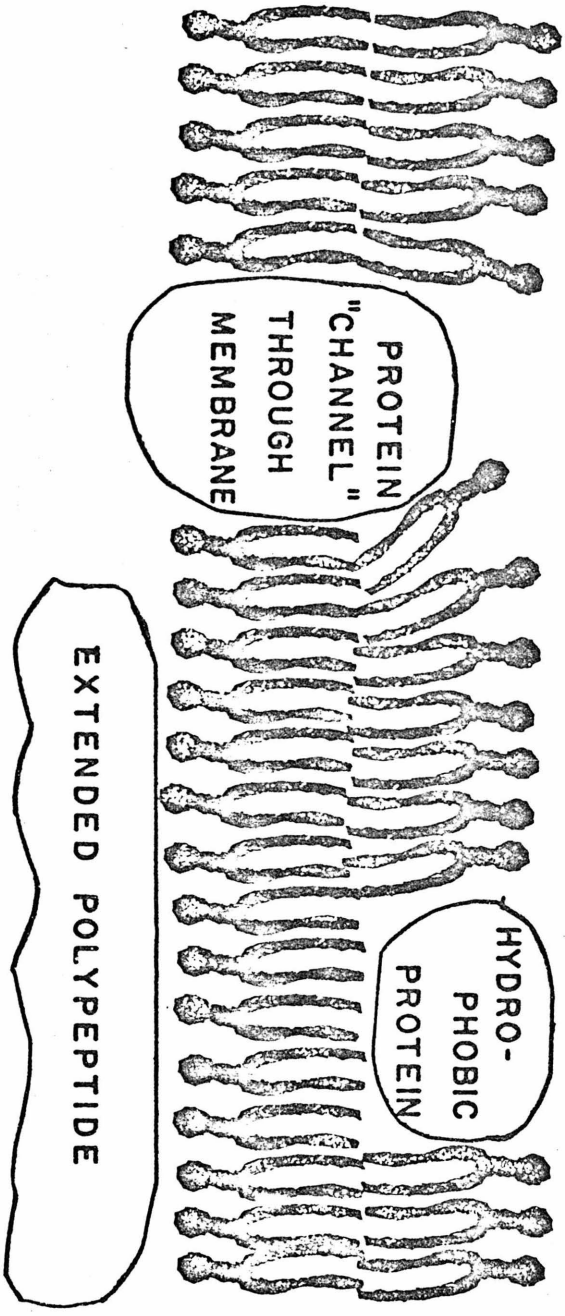
PROTEIN "CHANNEL" THROUGH MEMBRANE
HYDRO-PHOBIC PROTEIN
EXTENDED POLYPEPTIDE

level, e.g., is the protein on or inside the bilayer?, can be discussed in general, a greater degree of spatial resolution (questions of orientation, etc.) must be considered in reference to a specific membrane system. Since in physical studies of biological systems it is usually advisable to start with reasonably well known and characterized systems, further progress in membrane biophysics may depend on the availability of such systems, preferably systems which can be easily modified without severe functional disruption.

A system which has been chosen in Dr. S. I. Chan's laboratory as a possible candidate for long range studies is the inner mitochondrial membrane, and the work in part II is a contribution to this long range program and should be examined with a view to this larger context. The reasons for the choice of mitochondrial membranes as a system is primarily that simple reconstituted systems of purified components have been assembled which mimic quite accurately the properties of the intact membrane. It is therefore a reasonable hope that these mitochondrial membranes will serve as a bridge between the complex world of real cell membranes and the relatively simple world of pure phospholipid bilayers. Modern theories of the structure and function of the mitochondrial inner membrane will be treated now in some detail, since this system may be expected to assume a very important role in physical studies in the future. Furthermore, this survey will convey some idea of the complex mechanistic possibilities which arise in even the simplest realistic systems.

A Promising Molecular System: the Mitochondrial Inner Membrane

Two current pictures of the inner mitochondrial membrane[15, 16] are given in Fig. 4. Both pictures may be characterized as versions of the membrane model of Fig. 3, except that for inner mitochondrial membranes the protein components are known and identified,[17] and discussions of membrane structure can now be particularized to considerations of exact disposition of given proteins. In these pictures, FP represents a flavoprotein dehydrogenase which received electrons from the reduced form of nitocine adenine dinucleotide (NAD). At this stage of electron transport, called site I, the free energy of the reduction of FP is used to generate an adenosine triphosphate (ATP) molecule from adenosine diphosphate (ADP) and an inorganic phosphate ion (P_i). The electrons are passed, perhaps by means of coenzyme Q, to the cytochrome b/c_1 complex, site II, where another ATP is generated by the same type of coupled reaction. Cytochrome c then shuttles electrons to the cytochrome oxidase a/a_3 complex, called site III, where yet another ATP is generated, this time in a coupled reaction involving the reduction of molecular oxygen. The ATP produced by this system is essentially the molecular source of energy for all the biochemical processes of life. The overall scheme of reactions is shown in Fig. 5.

This reaction scheme is itself a factor in the formulation of the membrane models presented in Figs. 4 and 5. There are two popular models for the overall reaction mechanism of the

FIGURE 4

Mitochondrial inner membrane models. The model at the top has been proposed by adherents of the chemiosmotic hypothesis for the mechanism of oxidative phosphorylation, while that at the bottom was proposed by adherents of the chemical coupling hypothesis.

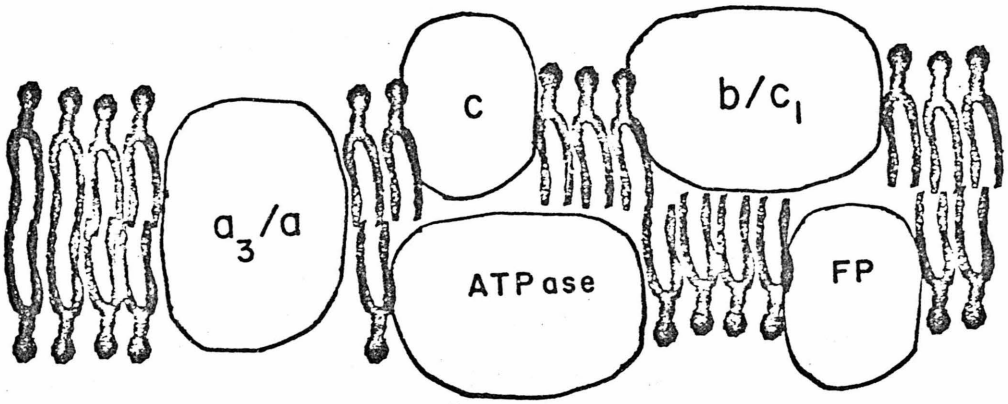
c
b/c1
a3/a
ATPase
FP

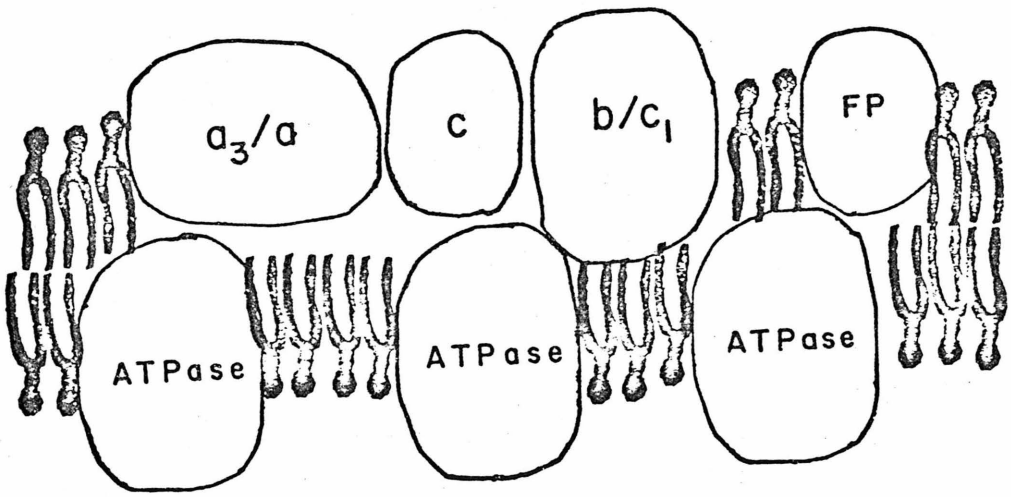
a3/a
c
b/c1
FP
ATPase
ATPase
ATPase

FIGURE 5

Pathway of Electron Transport in Mitochondria

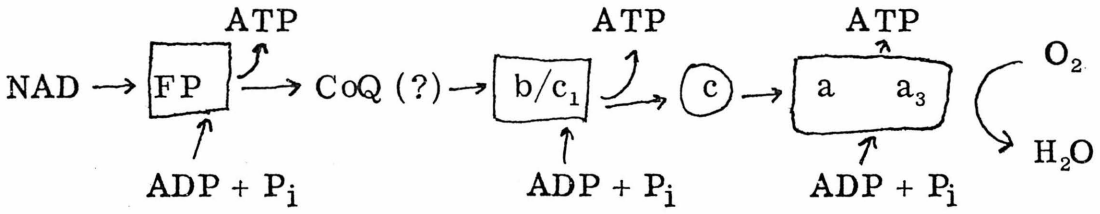

NAD	=	nicotine adenine dinucleotide
FP	=	flavoprotein
ATP	=	adenosine triphosphate
ADP	=	adenosine diphosphate
P_i	=	inorganic phosphate
b, c_1, c, a, a_3	=	cytochromes
CoQ	=	coenzyme Q

Electrons are passed from one molecule to the next, from left to right in this scheme, culminating in the reduction of molecular oxygen.

coupling of electron transport to ATP production, and the structural organization proposed by various authors largely depends on their position in this mechanistic debate. In one reaction scheme, the "chemical coupling" hypothesis,[18] electron transport is presumed to create reaction intermediated, for example, phosphorylated quinones[19] or histidine residues,[20] and that the phosphate is then transferred enzymatically to an ADP. The membrane serves in this scheme primarily to collect all the appropriate enzymes for the overall reaction in one place. In the other prominent reaction scheme, called the chemiosmotic hypothesis,[21] the process of electron transport is thought to create a potential gradient across the mitochondrial membrane, and this membrane potential is used to drive the usual ATP hydrolysis reaction in reverse. This scheme demands specific asymmetries in protein organization in the membrane, and predicts that oxidative phosphorylation will only occur in closed-membrane (vesicular) systems. The chemiosmotic hypothesis has gained in popularity recently, and compromise mechanisms[22] are currently being formulated.

Discussions of protein organization and reaction mechanism have been brought to an even simpler level by experiments on the reconstitution of the three sites of oxidative phosphorylation. Since this is the level of complexity at which physical experiments may be expected to yield the most detailed and powerful results, one of these experiments will be described here. It has been found possible[23] to reconstitute the third site of oxidative phosphorylation

in the following way: the cytochrome oxidase complex and a hydrophobic protein complex are sonicated in the presence of cytochrome c and a variety of purified lipids. The protein components are incorporated by this process into the resulting lipid bilayer vesicles. Cytochrome c is removed from the outside of the vesicles and a protein complex identified as an ATPase (called coupling factor F_1) is added to the vesicles. This simple system was capable of reducing molecular oxygen and generating ATP from ADP and P_i as a result.

This notable experiment has raised several questions which are possibly answerable by classical and modern methods of physical chemistry. First, it is found that the efficiency of this system depends on the amount and relative ratios of the lipids used, the lipids being phosphatidyl choline, phosphatidyl ethanolamine, and cardiolipin (Fig. 6). It is not clear whether these lipids exert direct electrostatic influences on the conformation of the protein involved, or whether the size and internal fluidity of the vesicles is more important. Second, an asymmetrical distribution of protein components in the vesicle (e.g., cytochrome c is removed from the outside) is necessary for the efficiency of the phosphorylation process. Thus many definite structural features of these vesicles are now determined and can be probed by physical techniques. In the hierarchy of levels of biological complexity shown in Fig. 7, the systems at level D are composed of only a few well characterized components but are able to mimic important processes

FIGURE 6

Structures of the main lipid components of mitochondrial inner membranes.

CARDIOLIPIN

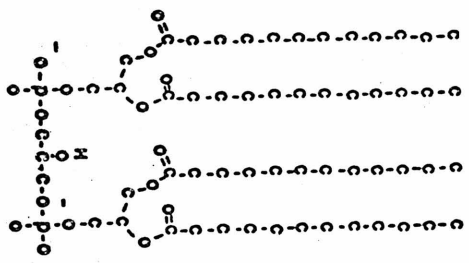

PHOSPHATIDYL CHOLINE

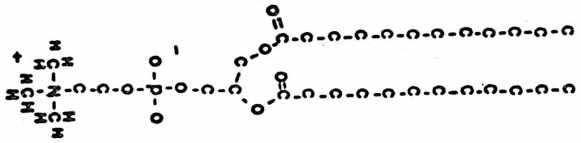

PHOSPHATIDYL ETHANOLAMINE

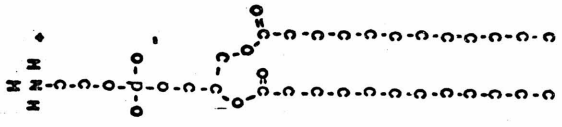

FIGURE 7

Level A	Real Cell Membranes *in vivo*
Level B	Intact Membranes *in vitro*
Level C	Membrane Fragments in suspension
Level D	Reconstituted Vesicle Systems
Level E	Phospholipid Bilayers

Hierarchy of levels of complexity of membrane and model membrane systems.

in the living cell. Therefore studies on this level may be directly relevant to the elucidation of actual biological mechanisms in vivo.

Since the components of these systems have generally been isolated and identified, many investigators have turned to spectroscopic studies, e.g., fluorescent probe methods,[17] electron paramagnetic resonance (epr),[24-27] or nuclear magnetic resonance (nmr),[28-33] in the hope of resolving questions of local mobility and organization of bilayer components. EPR studies of bilayers containing the cytochrome oxidase complex,[27] for example, have demonstrated that both bound lipids and free lipids exist in this system. Fluorescent probe studies of similar systems[17] have attempted to establish protein-protein distances in the reconstituted inner membrane complex. Finally, many investigators are also turning to nmr as a way of determining the structural consequences[29] of adding protein components to pure phospholipid systems. In view of this current interest, it is desirable here to review the two main forms of magnetic spectroscopy, epr and nmr, as these have proved to have notable advantages over other spectroscopic methods in the study of bilayer/protein organization.

The Magnetic Resonance Approach

An indication of the possible value of a form of spectroscopy may perhaps best be found by inspection of the Hamiltonian appropriate to the spectroscopic system being investigated. The electron

paramagnetic resonance and nuclear magnetic resonance Hamiltonians have interesting similarities and differences, and will be discussed together here partly because so many investigations of lipid bilayers use these techniques, and comparisons of the results of the different methods are often made.

The epr Hamiltonian[24] appropriate to an electron interacting with a single nuclear spin (this specialization is directed toward a discussion of the spin label[25] method in biophysics) may be written

$$\mathcal{H} = \beta \vec{H} \cdot \hat{g} \cdot \vec{S} + h \vec{S} \cdot \hat{A} \cdot \vec{I} \qquad (1)$$

where β is the Bohr magneton, h is Planck's constant, $\vec{H}$ denotes the applied magnetic field, $\hat{g}$ is a tensor which accounts essentially for all molecular perturbations of the value of $\vec{H}$ at the electron, $\vec{S}$ denotes the electron spin and $\vec{I}$ the nuclear spin, and $\hat{A}$, the hyperfine coupling tensor, accounts for the electron-nuclear coupling. This Hamiltonian has two properties of importance for investigation of local molecular environments and local mobilities, namely: (1) the values of the components of $\hat{g}$ and $\hat{A}$ are sensitive to local electronic structure, and (2) the Hamiltonian explicitly depends on the orientation of the molecule in the applied magnetic field, through the tensor couplings. If the orientation of the molecule fluctuates rapidly over all directions, as in a liquid, only an average g value will be observed. The tensor $\hat{A}$ is seen under these rapid tumbling conditions to consist of two parts, an

anisotropic hyperfine coupling tensor $\hat{T}'$, which accounts for the direct dipole-dipole interaction between the electron and nuclear spins, and an isotropic part $A_0 \cdot \hat{1}$ (where $\hat{1}$ is the unit tensor). The components of tensor $\hat{T}'$ are averaged to zero by isotropic tumbling and the average Hamiltonian becomes

$$\mathcal{H}_{av} = \beta g_{av} \vec{S} \cdot \vec{H} + h A_0 \vec{S} \cdot \vec{I} \quad . \tag{2}$$

This Hamiltonian no longer gives any indication of molecular orientations, but still contains information on local electronic structure.

The nmr Hamiltonian analogous to (1) for a pair of spins 1/2 can be written

$$\mathcal{H} = \sum_{1,2} - \hbar \gamma_i \vec{I}_i \cdot (\hat{1} - \hat{\sigma}_i) \cdot \vec{H} + \vec{I}_1 \cdot \hat{D}_{12} \cdot \vec{I}_2 + \vec{I}_1 \cdot \hat{J}_{12} \cdot \vec{I}_2 \tag{3}$$

where $\hat{\sigma}_i$ is the chemical shift tensor for nucleus i, $\hat{D}_{12}$ is the dipole-dipole coupling tensor between the nuclei, and $\hat{J}_{12}$ is the tensor representing the electron-coupled indirect nuclear spin interaction. In principle almost the same molecular information is obtainable from Eq. (3) as from Eq. (1); the tensor $\hat{1} - \hat{\sigma}_i$ is comparable to $\hat{g}$, $\hat{D}_{12}$ is comparable to $\hat{T}'$, and while $\hat{J}_{12}$ is itself in general not symmetric, this Hamiltonian goes to an average form

$$\mathcal{H}_{av} = \sum - \hbar \gamma_i (1 - \sigma_i) \vec{I}_i \cdot \vec{H} + J_{12} \vec{I}_1 \cdot \vec{I}_2 \tag{4}$$

for molecules rapidly tumbling in solution.

The information obtainable in practice from Eqs. (1) and (3) depends on the value of the tensor components. For example, a nitroxide moiety in a dimethyloxazolidine ring (a typical and popular spin label) (Fig. 8) has an epr spectrum dominated by the anisotropic part of $\hat{A}^{(26)}$ (i.e., $\hat{T}'$) at an external field strength of 3.3 kG, when the spin label does not tumble freely. Motional information is extracted from such spectra by calculating the average $\hat{T}'$ over different motions and comparing observed spectra to those predicted for different $\hat{T}'_{av}$. Likewise, the nmr spectrum of a pair of geminal proton spins on an alkyl chain undergoing restricted motion will be completely dominated by $\hat{D}_{12}$, and the spectrum will give motional information through consideration of the $\hat{D}_{12av}$ needed to produce such spectra.

The main advantage of the epr spin label method of investigating local mobilities has been that the spectrum of the spin label is simple and the interpretation of spectra relatively straightforward. The crucial disadvantage of this technique is that the spectrum tells the mobility of the spin label, not the mobility of the unperturbed molecule of interest. The spin label itself is usually reasonably bulky (see Fig. 8), and experimental results from this technique in studies of lipid bilayers may be misleading (as is shown later in this thesis) because of the severity of the spin label's perturbation of local chain packing.

The situation in nmr investigations is frequently the reverse of this. The nmr method introduces no perturbation on the

FIGURE 8

The structure of a typical "spin-labelled" fatty acid.

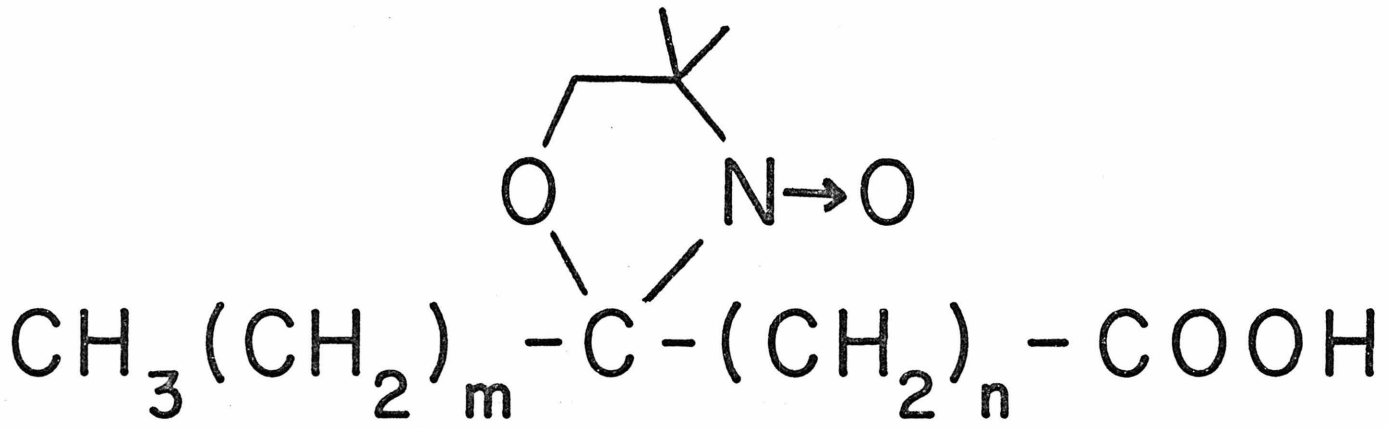
O
N→O
CH3(CH2)m-C-(CH2)n-COOH

system at all, but the spectrum will often be complicated and difficult to interpret. Spectral simplification, however, can frequently be effected by substituting particular nuclei (^{2}H and ^{19}F for protons, ^{13}C for carbon) which constitute a very slight perturbation of the system being studied.

Recent advances[34, 35] in the nmr of solid samples have also begun to give nmr an additional advantage over epr in motional investigations. Pulse methods have been developed which allow the term $\vec{I}_1 \cdot \hat{D}_{12} \cdot \vec{I}_2$ to be averaged rapidly to zero without eliminating the other terms in the magnetic Hamiltonian (3). This method produces a spectrum dominated by $(\hat{1} - \hat{\sigma})$ and $\hat{J}_{12}$, and these terms will be sensitive, in general, to slower motions than those affecting $\hat{D}_{12}$. Thus an nmr study, using this technique, can discriminate motions occurring on a wide range of timescales, and can make use of different averaging properties of the tensors in Eq. (3) to check its conclusion.

The papers presented here, however, use the simpler method of studying the averaging of $\hat{D}_{12}$ by local molecular motions. These studies exploit the fact that many lipid bilayer systems contain essentially two kinds of protons, methyl protons and alkyl chain methylene protons, and that the resulting spectra are reasonably simple. Even these simple spectra have proved controversial, and a discussion of the status of magnetic resonance studies of lipid bilayers is appropriate here.

NMR Studies of Bilayers

The understanding of the state of molecular motion of lipids in bilayers, both sonicated and unsonicated, has been the goal of numerous nmr studies.[30, 31] In general these studies have suffered from two coupled drawbacks. First, ordinary high resolution nmr spectrometers cannot observe the broad proton nmr lines (~ 3,000-4,000 Hz) characteristic of unsonicated lipid bilayers, and most investigators have turned to sonicated systems, which exhibit sharp (~ 5-20 Hz) proton resonances. Second, in the absence of an adequate theory to describe the nmr linewidth of spins undergoing restricted local motions and slow overall tumbling, many investigators decided that overall vesicle tumbling alone[32] was sufficient to produce the observed line narrowing upon sonication, and that bilayers in general could be said to have a fluid local structure. This interpretation was questioned by other workers,[33] who found that changing the effective tumbling rate of the vesicles by changing solution viscosity produced negligible changes in the lipid proton linewidths. These authors proposed that the local packing of lipids is perturbed in the sonicated structures (Fig. 9) and that the motional freedom of the lipids is significantly different in the sonicated and unsonicated systems.

This controversy has both applied and theoretical aspects of importance. Cell membranes have dimensions much more like those (microns or greater) of unsonicated bilayers than sonicated

FIGURE 9

Sonicated bilayer vesicle (right) and unsonicated multilayers of bilayers (left).

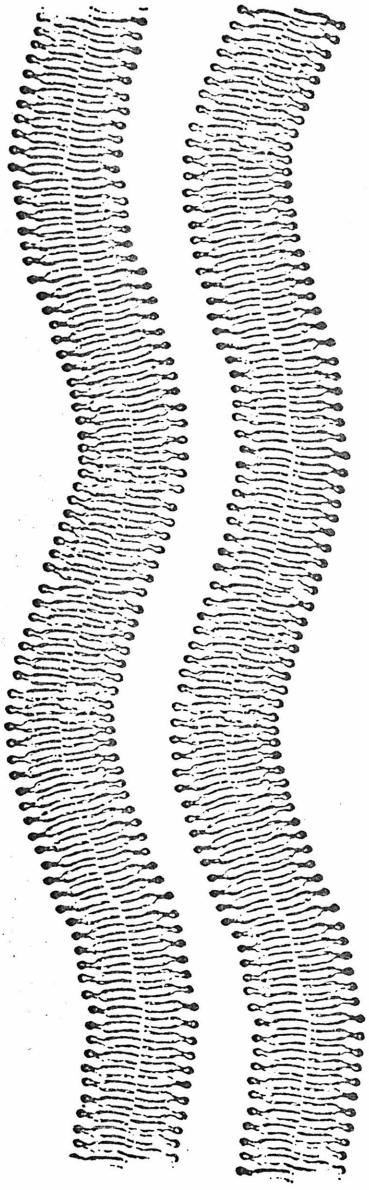

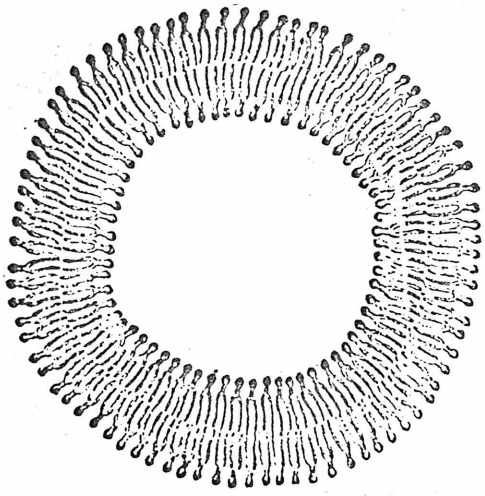

vesicles, and if it is shown that small (250 Å) vesicles have severely disturbed local lipid packing, then these vesicles may be expected to give little relevant information about the state of lipids in real biomembranes. Furthermore, understanding of the relative line-narrowing effects of overall tumbling and local restricted motion is critical in interpreting not just spectra of simple bilayers but spectra of proteins and most other biological macromolecules as well. Very little progress in the nmr of large aggregates in solution or bound to membranes could be expected without an adequate theory of this type, and the second paper presented in this thesis is a contribution towards such a theory. Since this topic is so central to an understanding of the nmr spectra of complex biological systems, an intuitive treatment of motional narrowing will now be presented.

NMR Linewidth and Complex Motions

The proton nmr spectrum of a rigid solid, for example a block of paraffin, has a linewidth (width at half signal height) of tens of thousands of Hz. This width, due almost exclusively to dipole-dipole coupling between the proton spins, can be called $|\Delta H_{loc}|$, because it represents the variation in local field throughout the sample due to the magnetic fields of the dipole spins themselves. It has been shown[36] that, if the paraffin molecules were now allowed to tumble freely in space with a motional correlation time τ_c, the resulting nmr linewidth could be calculated as

$$\Delta\nu \sim \gamma^2 \left| \Delta H_{loc} \right|^2 \cdot \tau_c \quad , \tag{5}$$

where γ is the proton gyromagnetic ratio, as long as τ_c is small compared to $1/\gamma \left| \Delta H_{loc} \right|$. That is, free isotropic tumbling on a timescale of 10^{-5} seconds starts to give a narrowed nmr line, which is narrowed even further for faster motions.

A more difficult question now arises: suppose in the paraffin restricted local molecular motions had already produced a somewhat narrowed line, compared to a rigid solid. This new linewidth is described by a new field variation $\left| \Delta H'_{loc} \right|$, and little chunks of this paraffin are now tumbled isotropically on some timescale τ_c. What linewidth results in this case? The natural impulse to use the formula

$$\Delta\nu \sim \gamma^2 \left| H'_{loc} \right|^2 \cdot \tau_c \tag{6}$$

has been followed[35, 36] on several occasions in the literature on bilayers, where just such a problem arises. If this approach were correct, then the much narrower lines observed for sonicated as compared to unsonicated bilayers could be attributed to sonicated vesicle tumbling rather than local increase of molecular disorder upon sonication. Equation (6), however, turns out to be a good approximation only in a few rather unphysical cases, as a closer examination of dipolar broadening will now show.

The usual truncated dipolar Hamiltonian for a pair of protons is written

$$\mathcal{H}_0 = \gamma^2 \hbar^2 \frac{(1 - 3\cos^2\theta_{12})}{r_{12}^3} \cdot \left[I_{1Z} \cdot I_{2Z} - \tfrac{1}{4} (I_1^+ I_2^- + I_1^- I_2^+) \right] \quad (7)$$

where r_{12} is the magnitude of the internuclear vector $\vec{r}_{12}$, θ_{12} is the angle between $\vec{r}_{12}$ and the applied magnetic field $\vec{H}_0$, and I_Z, I^+, and I^- have their usual meanings as spin operators. This Hamiltonian may be thought of as a small perturbation on the Zeeman Hamiltonian

$$\mathcal{H}_Z = -\gamma \hbar H_0 (I_{1Z} + I_{2Z}) \quad (8)$$

where the effects of chemical shift and chemical shift anisotropies discussed earlier may be suppressed for clarity. The Hamiltonian $\mathcal{H}_Z$ would give rise to an nmr spectrum consisting of a single line at frequency ω_0. The perturbation H_0 splits this single line into two broadened lines: the splitting is induced by the term in $I_{1Z} \cdot I_{2Z}$ and the broadening by the exchange term $(I_1^+ I_2^- + I_1^- I_2^+)$. In a sample containing many pairs of spins at different orientations and different values of r_{12}, the resulting spectrum of the solid sample is as shown in Fig. 10c. If local restricted reorientation of the spin pairs produces modulation of the values of $(1 - 3\cos^2\theta_{12})$, the partially narrowed spectrum shown in Fig. 10d results. This modulation also produces an average uncertainty in the value of $(1 - 3\cos^2\theta_{12})$ which gives an additional contribution to the width of the sub-lines underlying the whole spectrum. If the local motions are fairly extensive, this broadening will be more important than the original quantum exchange broadening, which is reduced

FIGURE 10

Schematic illustration of nmr linewidth situations.

(a) A solid sample of isolated spins gives a single resonance line.

(b) A solid sample of pairs of spins, all with the same orientation, gives a pair of quantum exchange broadened lines.

(c) A solid sample of coupled spins gives a wide "rigid lattice" spectrum.

(d) Restricted local motions of the spins in the solid sample produce a partially narrowed line compared to (c). The lineshape is an envelope of lines whose width is determined by the local motions.

(e) The sample in (d) is broken up into chunks which tumble in solution, retaining the same local motion. If the tumbling is slow compared to the local motions, the minimum linewidth which results is that of the sub-lines in case (d).

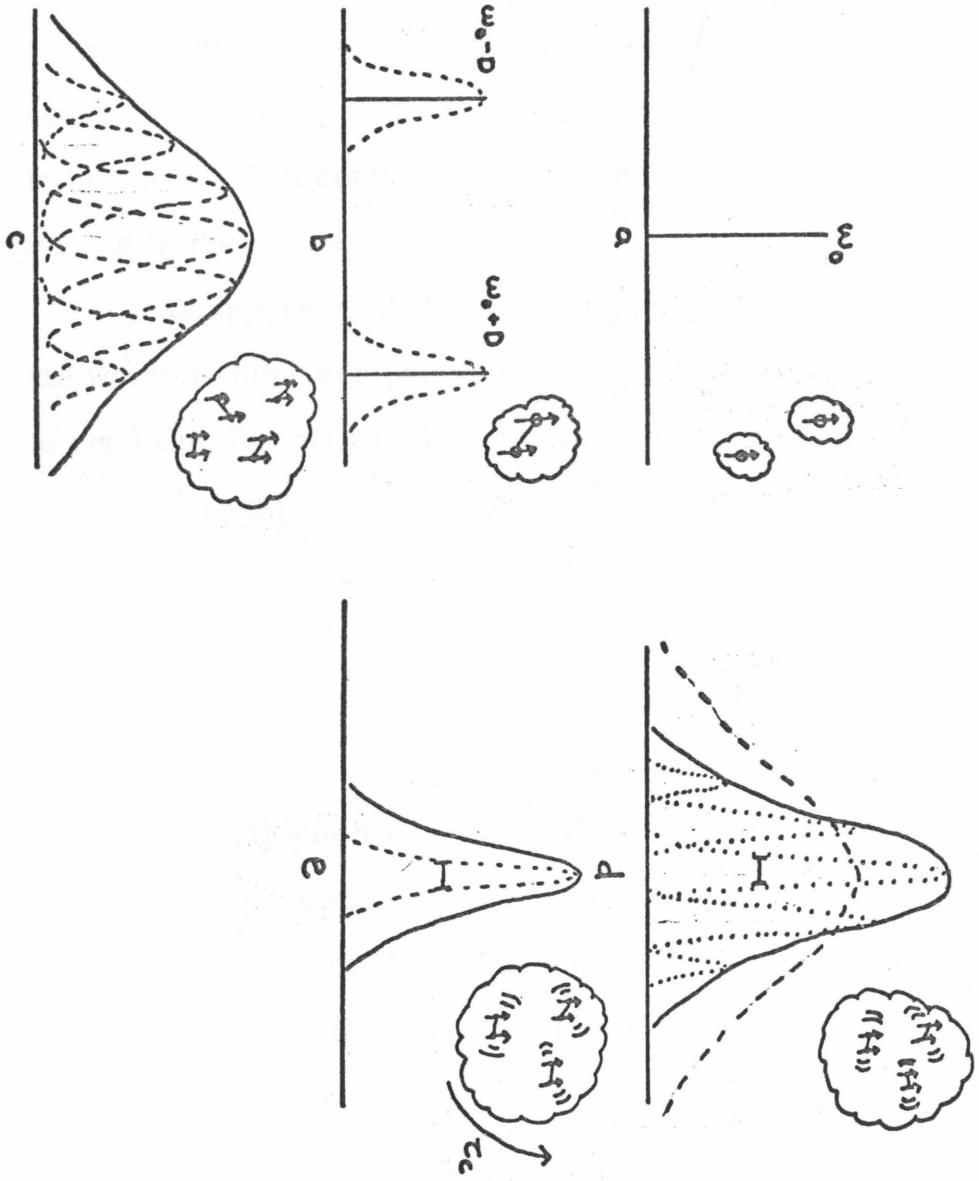
a
ε_0
b
ε_0-D
ε_0+D
c
d
I
e
I
τ_c

by the additional motion. Thus the situation for a sample of protons such as those in unsonicated lipid bilayers is like that shown in Fig. 10d. The dipolar interaction is not completely averaged out by the restricted local motion possible for the spins, and this produces a certain spread of resonance lines. Each of these lines furthermore has a certain width caused by the local motional fluctuations in the dipolar interaction.

It is apparent, that if the spins are now also tumbled at a rate which is slow compared to the rate of these local motions, the resulting line will be at least as broad as the "local motional width" in the static case. This is essentially the same phenomenon as the so-called $T^{\dagger}$ or $T_{1\rho}$ broadening in multiple-pulse nmr, where the rate of repetition of the averaging-pulse cycle may be slow compared to the rate of various local motions. In a complete treatment, the linewidth upon tumbling is found to be greater than this minimum "local width", because of the details of averaging $(1 - 3\cos^2\theta_{12})$ factors, as is proved later in this thesis.

A variation of Eq. (6) which has been proposed[37] to account for "local width" difficulties has the form

$$\Delta\nu \sim A^2 \cdot \tau_c + B^2 \cdot \tau_{loc} \qquad (9)$$

where A^2 is an analog of $|\Delta H'_{loc}|^2$, B^2 is essentially $|\Delta H_{loc}|^2 - |\Delta H'_{loc}|^2$, and τ_c is a vesicle tumbling time. This simple relation is unfortunately also inadequate for the linewidth problem in sonicated systems. The real physical situation experienced by a

proton spin in a sonicated bilayer is that it sees a local field fluctuating through the complete range of local fields possible in the sample (i.e., $|\Delta H_{loc}|$) and this fluctuation, if Fourier analyzed, would prove to have significant frequency components at $\omega_1 = 1/\tau_c$, $\omega_2 = 1/\tau_{loc}$, and $\omega_3 = 1/\sqrt{\tau_c \tau_{loc}}$. This last frequency arises because two different processes, tumbling and local motion, are producing time variations in the same quantity $(1 - 3\cos^2\theta_{12})$. That is, a single local field fluctuating with a complex set of correlation times must be analyzed, rather than two "effective" local fields each with its own characteristic fluctuation time.

Under the condition that τ_{loc} were infinitely fast, both Eqs. (6) and (9) and the expression presented later in this thesis reduce to the same form, because this would represent a pseudo-static partially narrowed case, in which the "local widths" were zero and the partially narrowed spectrum in Fig. 10d would be an envelope of perfectly sharp lines. Investigators have been encouraged to use forms like Eqs. (6) and (9) by their assumption that the local motions of lipid chains were extremely rapid, and the equations themselves have the treacherous property of returning this assumption back to the researcher disguised as a result.

A main part of this thesis is devoted to establishing a correct linewidth expression for this situation which has caused great confusion. The two papers presented here represent essentially the experimental and the theoretical aspects of the resolution

of these local motional problems, with special emphasis on the role of methyl groups in the elucidation of local molecular mobilities. The first paper is an exposition of the delayed Fourier transform (DFT) technique, which was developed in Dr. S. I. Chan's laboratory to allow separate observation of the methyl and methylene proton resonances in bilayers. The intensity anomaly of the methyl resonances reported in this paper motivated much of the detailed linewidth analysis of the second paper. This first paper also reports the first application, by Dr. M. C. Hsu, of the DFT method to studies of protein-bilayer interactions, a subject which has been characterized in this Introduction as a main goal of the bilayer work in this laboratory.

The second paper presents the details of the linewidth, and for methyl groups more accurately the lineshape, analysis relevant to proton nmr spectra of sonicated and unsonicated lipid bilayers, and discusses the difference in local structure which nmr is able to detect in these two systems. In addition it provides a brief introduction to Anderson linewidth calculations in general, in the hope of encouraging application of these calculations to systems of biological interest.

REFERENCES

1. E. Gorter and F. Grendel, J. Exp. Medicine, 41, 439 (1925).
2. J. F. Danielli and E. N. Harvey, J. Cell. Comp. Physiol., 5, 483 (1935).
3. H. Davson and J. F. Danielli, "The Permeability of Natural Membranes" (2nd ed.), London, Cambridge University Press, 1952.
4. F. O. Schmidt, R. S. Bear and K. J. Palmer, J. Cell Comp. Physiol., 18, 31 (1941).
5. J. B. Finean, Int. Rev. Cytol., 12, 303 (1961).
6. J. E. Thompson, R. Coleman and J. B. Finean, Biochim. Biophys. Acta, 150, 405 (1968).
7. S. Knutton, J. B. Finean, R. Coleman and A. R. Limbrick, J. Cell Sci., 7, 357 (1970).
8. M. H. F. Williams, A. E. Blaurock and D. M. Engelman, Nature, New Biol., 230, 72 (1971).
9. J. D. Robertson, J. Biophys. Biochem. Cytol., 3, 1043 (1957).
10. D. M. Engelman and W. Stoeckenius, J. Cell Biol., 42, 612 (1969).
11. J. B. Finean, T. A. Bramley and R. Coleman, Nature, 229, 114 (1971).
12. D. E. Green and J. F. Perdue, Proc. Nat. Acad. Sci., 55, 1295 (1966).
13. P. Mueller, D. O. Rudin, H. T. Tien and W. C. Wescott,

Nature, 194, 179 (1962).

14. P. Mueller and D. O. Rudin, Biochem. Biophys. Res. Commun., 26, 398 (1967).
15. J. M. Palmer and D. O. Hall, in "Prog. Biophys. Mol. Bio.", 24, 125 (1972).
16. A. L. Lehninger,"Bioenergetics", Menlo Park, 1971.
17. E. Racker, in "Essays in Biochemistry" (P. N. Campbell and F. Dickens, eds.), Academic Press, London, Vol. 6, p. 1, 1970.
18. V. Massey and C. Veeger, Ann. Rev. Biochem., 32, 579 (1963).
19. A. F. Brodie and P. J. Russell, Proc. 5th Int. Cong. Bioch. Moscow, Oxford Pergamon, 5, 89 (1961).
20. P. D. Boyer, Science, 141, 1147 (1963).
21. P. Mitchell, Biol. Rev., 41, 445 (1965).
22. E. Racker, in "Structure and Function of Membranes of Mitochondria and Chloroplasts", E. Racker, ed., Reinhold, New York, p. 127, 1969.
23. E. Racker and A. Kandrach, J. Biol. Chem., 248, 5841 (1973).
24. J. E. Wertz and J. R. Bolton, "Electron Spin Resonance", McGraw Hill, New York, 1972.
25. S. Ohnishi and H. M. McConnell, J. Amer. Chem. Soc., 87, 2293 (1965).
26. W. H. Hubbell and H. M. McConnell, Proc. Nat. Acad. Sci., 64, 20 (1969).
27. P. Jost, O. H. Griffith, R. A. Capaldi and G. Vanderkooi,

Biochim. Biophys. Acta, 311, 141 (1973).

28. D. Chapman, D. J. Flack, S. A. Penkett and G. G. Shipley, Biochim. Biophys. Acta, 163, 255 (1968).
29. Y. K. Levine, Prog. Biophys. Mol. Bio., 24, 1 (1972).
30. E. G. Finer, A. G. Flook and H. Hauser, Biochim. Biophys. Acta, 260, 59 (1972).
31. M. P. Sheetz and S. I. Chan, Biochemistry, 11, 4573 (1972).
32. Z. Veksli, N. J. Salsbury and D. Chapman, Biochim. Biophys. Acta, 183, 434 (1969).
33. E. G. Finer, A. G. Flook and H. Hauser, Biochim. Biophys. Acta, 260, 49 (1972).
34. R. W. Vaughan, Ann. Rev. Mat. Sci., 4 (to appear 1974).
35. U. Haeberlen and J. S. Waugh, Phys. Rev., 175, 453 (1968).
36. R. Kubo and K. Tomita, J. Phys. Soc. Japan, 9, 888 (1954).
37. E. G. Finer, private communication.

PART II

A. DELAYED FOURIER TRANSFORM PMR SPECTROSCOPY

Abstract

Broad resonances may be filtered out of Fourier transform pmr spectra by introducing a data collection day after each rf pulse. This filtering makes possible accurate intensity and position measurements on narrower resonances in spectra which contain both broad and narrow components. The crystalline $\rightleftharpoons$ bilayer phase transition of dipalmitoyl lecithin and the behavior of egg lecithin bilayers upon addition of valinomycin have been monitored using this technique.

We describe here a simple modification of standard Fourier transform (FT) nmr methods[1] which may be used in analyzing spectra which contain both broad and narrow components. Frequently, linewidth and intensity measurements on the narrower resonances of such spectra are difficult, because these peaks appear superimposed against the broader resonances. It is possible, however, to filter out the broad resonances from the spectrum, by introducing a delay time between the end of the rf pulse and the start of data collection. Each component of the transient signal will then have decayed to exp $(-\Delta\tau/T_2)$ of its initial value

by the time the recording of the transient begins. Here $\Delta\tau$ is the length of the pulse plus the chosen delay time, and T_2 is the transverse relaxation time associated with a given component. The resulting transformed spectrum will then exhibit all the components present in the usual continuous wave (CW) nmr spectrum, but with each component weighted by its own factor exp $(-\Delta\tau/T_2)$. The effect of this weighting process on lines of various widths is shown in Table I.

The advantage of this filtering effect may be seen in our recent nmr work on unsonicated lecithin bilayers. A typical CW nmr spectrum for the protons in a sample of egg lecithin bilayers is shown in Fig. 1a. This spectrum reveals several narrow components, but the bulk of the signal is very broad, and obscures the sharper resonances, making it difficult to determine their spectral position and intensity. A delayed Fourier transform (DFT) spectrum of dipalmitoyl lecithin at 100 MHz and at 60°C with $\Delta\tau$ set at 500 μsec is shown in Fig. 1b. In this spectrum the broad component in the usual CW spectrum can be seen to be essentially completely "filtered", and the narrower components can be readily monitored.

The DFT technique has enabled us to monitor the crystalline $\rightleftharpoons$ bilayer transition in dipalmitoyl lecithin. Above 42°C, dipalmitoyl lecithin forms a bilayer dispersion in excess D_2O, but below this temperature it exhibits a crystalline phase.[2] For the crystalline phase, the DFT spectrum revealed no sharp

TABLE I

The selective filtering effect of a data-collection-delay time $\Delta\tau$ = 500 μsecs on nmr lines of various widths in Fourier transform nmr spectroscopy

$1/\pi$ T_2 Hz	fraction of magnetization remaining
10	0.98
50	0.92
100	0.85
200	0.73
500	0.46
1000	0.21
2000	0.04

FIGURE 1

High resolution pmr spectra of aqueous lecithin bilayer samples: (a) 220 MHz CW spectrum of egg lecithin bilayers at 29°C; (b) 100 MHz delayed Fourier transform spectrum of dipalmitoyl lecithin bilayers at 60°C. The peak centered at -1.14 ppm is assigned to terminal methyl groups on the hydrocarbon side chains of the lecithin molecule. The resonance at -3.32 ppm is from choline methyls of the ionic head groups. The residual protons in the solvent (D_2O) appear at -4.48 ppm. The peak at -6.42 ppm is a calibrated intensity standard of chloroform doped with the free radical, 2, 2-diphenyl-1-picrylhydrazyl. Chemical shifts are referred to external TMS (10% in carbon tetrachloride).

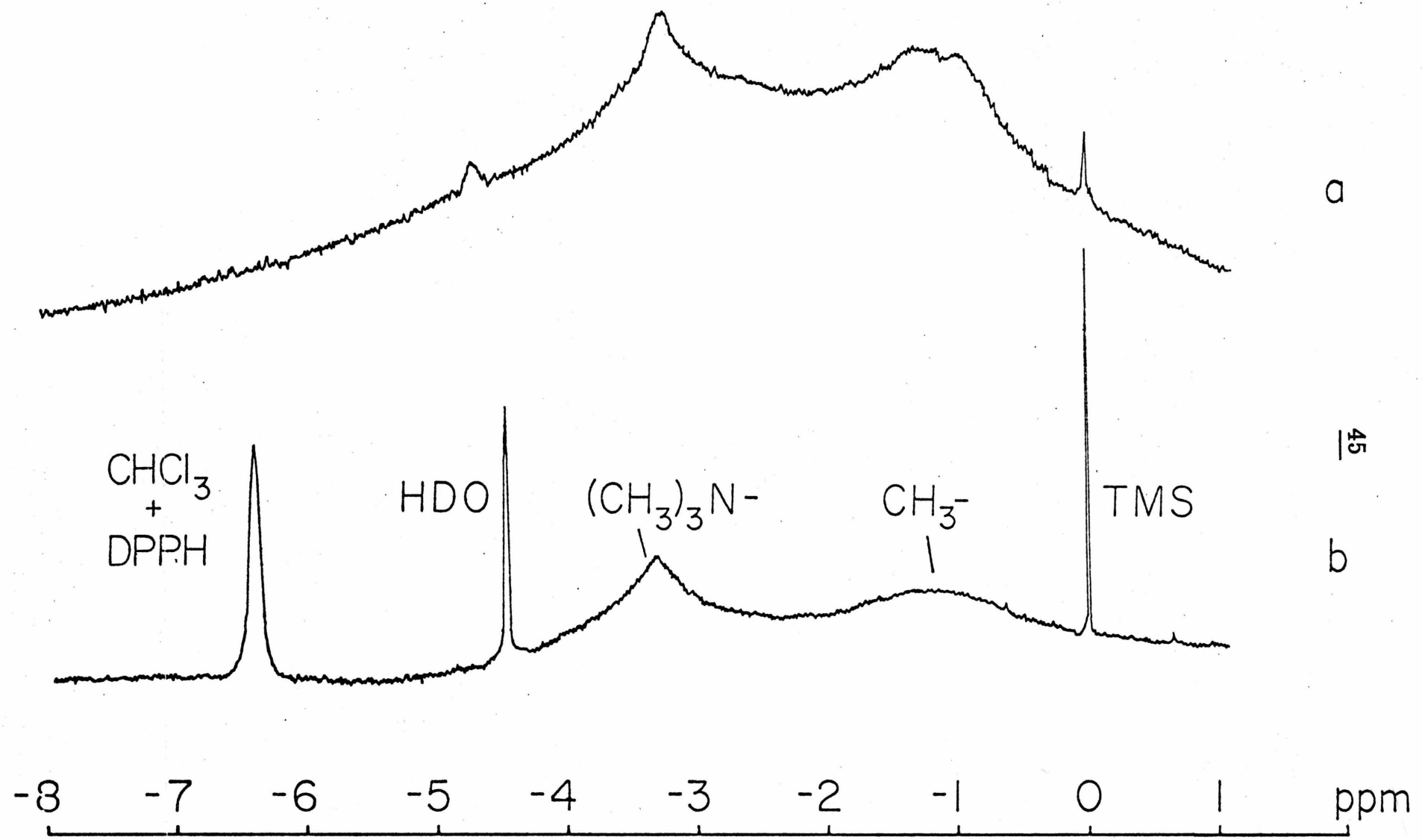
a
b
45
CHCl3
+
DPPH
HDO
(CH3)3N-
CH3-
TMS
-8
-7
-6
-5
-4
-3
-2
-1
0
1
ppm

components. The DFT spectrum above the phase transition is depicted in Fig. 1b. The spectral intensities of the choline methyl and terminal methyl resonances are plotted as a function of temperature in Fig. 2. These intensities are presented as a percentage of the expected intensity of each chemical species, calculated from the species' molarity in the sample. It can be seen from Fig. 2 that both the choline and terminal methyl groups are simultaneously mobilized near the bilayer phase transition temperature.

Changes in the lipid bilayer pmr spectrum upon addition to the bilayer of ion-specific transport carriers such as the cyclic oligopeptide antibiotic, valinomycin, can also be observed by this technique. In Table II is displayed the effect of valinomycin, in the amount one molecule of valinomycin per fifty lecithin molecules, in an egg lecithin bilayer dispersion. We observed that the addition of valinomycin reduces the linewidth of the choline methyl resonance by 50% but has little effect on the resonance of the terminal methyl groups. The intensity of the choline methyl resonance is also reduced by 50%. These results suggest that valinomycin interacts with the bilayer predominantly at the polar head region.[3]

These examples illustrate the value of DFT nmr in distinguishing peaks which are difficult to analyze in ordinary CW nmr spectra because they appear against a background of stronger and broader resonances. This method also allows the measurement of T_1 as well as T_2 of these otherwise obscured lines by the

FIGURE 2

Variation of the choline and terminal methyl signal intensities with temperature for a dipalmitoyl lecithin bilayer sample, using delayed Fourier transform pmr at 100 MHz.

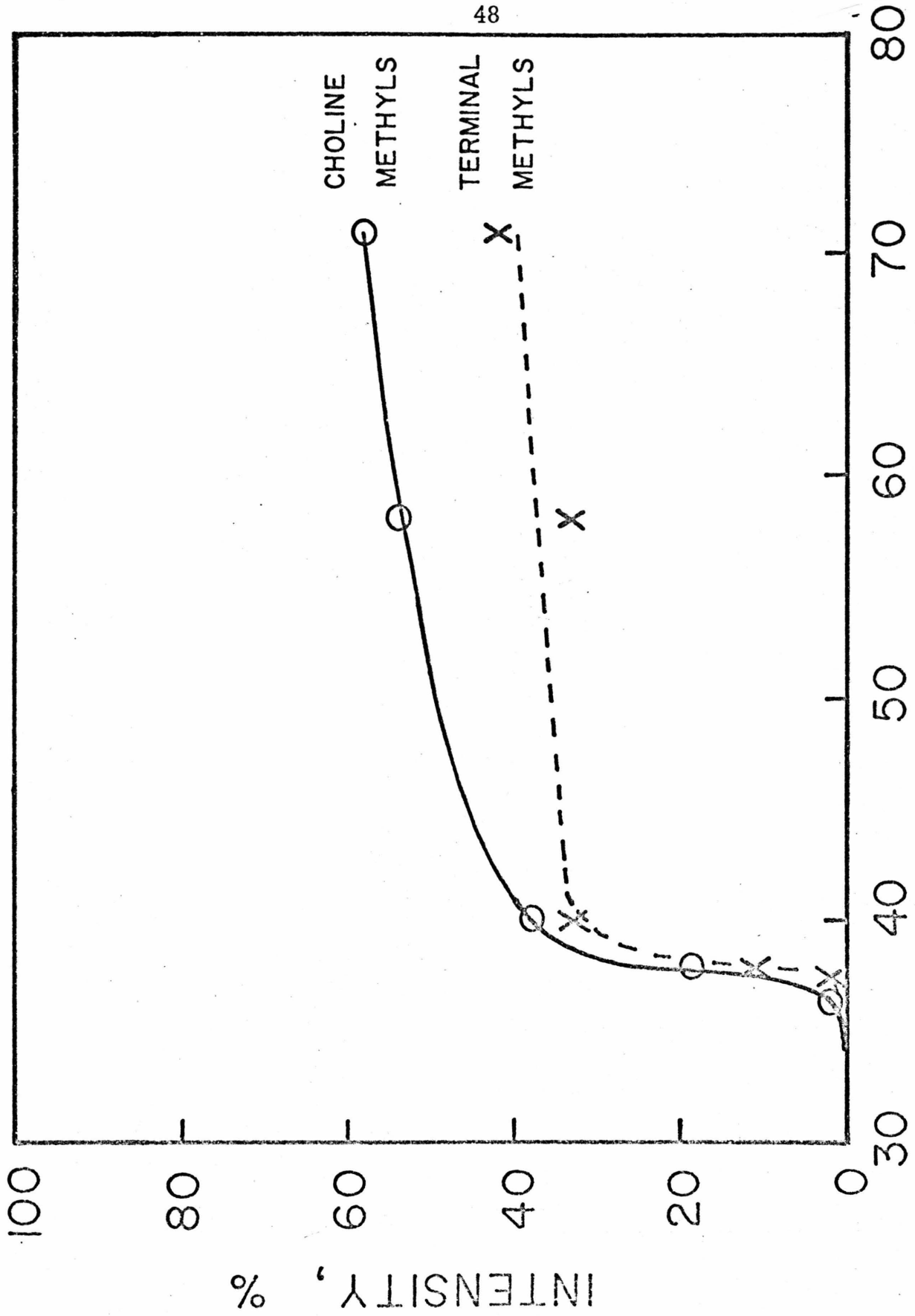
CHOLINE METHYLS
TERMINAL METHYLS
INTENSITY, %
TEMPERATURE, °C
0
20
40
60
80
100
30
40
50
60
70
80

TABLE II

The effect of valinomycin on the DFT pmr spectrum[a] of an egg lecithin water dispersion

	Lecithin		Lecithin + 2% Valinomycin	
	choline methyl	terminal methyl	choline methyl	terminal methyl
Linewidth	120 Hz	160 Hz	68 Hz	160 Hz
% of protons observed	30%	50%	17%	50%

[a] 100 MHz

method of Freeman and Hill.[4] We have, for example, recently determined the T_1's and the linewidths of both the choline and terminal methyls of egg lecithin bilayers.[5] Hopefully, further applications can be made to nmr studies of liquid-crystalline and gel-like samples in general.

REFERENCES

1. R. R. Ernst and W. A. Anderson, Rev. Sci. Instr., 37, 93 (1966).
2. D. Chapman, R. M. Williams, and B. D. Ladbrooke, Chem. Phys. Lipids, 1, 445 (1967).
3. S. M. Johnson and A. D. Bangham, Biochim. Biophys. Acta, 193, 82 (1969).
4. R. Freeman and H. D. W. Hill, J. Chem. Phys., 54, 3367 (1971).
5. G. W. Feigenson and S. I. Chan, J. Amer. Chem. Soc., in press.

B. MOLECULAR MOTION IN LIPID BILAYERS: AN NMR LINEWIDTH STUDY

Abstract

A model of the molecular motional state of unsonicated lipid bilayers is derived from proton magnetic resonance (pmr) linewidth considerations. The pmr linewidths of both chain protons and the protons of methyl groups are calculated using a computer program based on P. W. Anderson's stochastic theory of resonance linewidths. Spin-lattice relaxation phenomena observed for protons in lipid bilayers are also explained in terms of the same motional model. Finally, the effects of sample sonication on the pmr linewidths are discussed in the light of stochastic relaxation results.

Introduction

Amphiphilic molecules, e. g., soaps, lecithins, or surfactants generally, can form bilayer structures in water resembling those found in cell membranes.[1-6] Recently many biologically motivated studies of these lipid bilayers[7-18] have tried to determine the degree of molecular mobility in the interior and at the surface of the bilayer. Although proton magnetic resonance (pmr) would be a natural tool for such mobility studies, efforts thus far have been hampered by lack of an adequate treatment of the unique

motional averaging effects which are found in nmr spectra when molecular motion is significantly restricted.

These restricted motion effects may be seen most clearly in experiments performed on samples in which bilayer sheets are oriented parallel to glass plates.[14, 15] The linewidth of the pmr signal arising from the hydrocarbon chain protons in these bilayers depends strongly on the angular orientation of the sample in the external magnetic field. This demonstrates that the motion of these chains in the interior of the bilayer is seriously restricted. It also shows the pmr linewidth of the protons on these chains to be purely dipolar in origin. The details of this angular dependence suggest that chain proton pairs can execute rapid (faster than 10^{-5} sec) motions about the chain axis. There must, however, be other types of motion present as well, since the chain proton linewidth (3000-6000 Hz) in the spectra of unoriented bilayers is narrower than would be expected from this type of motion alone. In this connection, it should be noted that the tumbling correlation time of unsonicated bilayer sheets is too long to produce any motional narrowing at all.

Since internuclear vectors between protons on the lipid molecules thus cannot tumble freely over all directions in space (this is the exact meaning of "restricted" in this context), the usual linewidth expression appropriate to isotropic, liquid-like systems, cannot be used here. Rather, a treatment of the pmr spectra exhibited by lipid bilayers must start with the rigid

lattice powder spectra of these bilayers with the effects of various degrees of restricted local motion then introduced.

The only practical method for calculating such effects is the stochastic linewidth theory of Anderson,[19] or specifically the Monte Carlo version of this theory used by Saunders and Johnson.[20] Since this theory correctly describes all linewidth effects arising from motions whose correlation times are long compared to $1/\omega_0$ (ω_0 is the resonance frequency of the signal), this type of calculation can predict the results of any sort of motion, including isotropic as a special case.

Many amphiphilic molecules also contain, in addition to the methylene chain protons, both chain terminal methyl protons and methyl protons in the hydrophilic or polar region of the molecule. The pmr spectra of such molecules (e.g., lecithins, alkyl-trimethyl ammonium soaps) show relatively narrow methyl peaks, around 200 Hz in linewidth compared to 3000 Hz for methylene protons, which have significantly less intensity than would be expected from the methyl proton concentration in the sample.[21] These two observations can also be explained in terms of restricted motion effects. The Anderson theory can be used to introduce motional averaging into the powder spectrum of the three-spin group in this case.

Although Anderson's theory is well known to relaxation specialists, its application to the nmr of biological systems is novel and requires care in the definition of certain concepts.

This paper therefore proceeds in three parts. The first part is a discussion of the Anderson theory and the terminology of motional narrowing as background for non-specialists. Next, the application of this theory to pmr linewidths observed in unsonicated lipid bilayers is discussed in detail, and the motional model which emerges from this treatment is examined in the light of spin-lattice relaxation results. Finally, the theory is modified to allow a treatment of the effects of sample sonication on lipid bilayer pmr linewidths.

Method

Anderson showed that, for a resonance signal whose spin-spin relaxation rate T_2 is fast compared to its T_1, the free induction decay $g(t)$[22] associated with that resonance may be computed from the expression

$$g(t) = \overline{\exp\left(i \int_0^t \omega(\tau)\, d\tau\right)} \qquad (1)$$

Here $\omega(\tau)$ is the resonance frequency of the transition and the bar denotes averaging over an ensemble of spins. In general, $\omega(\tau)$ is time-dependent because of fluctuating local magnetic fields (dipolar, anisotropic chemical shift, etc.).

The above expression is best understood by considering a few familiar applications. The case of a spin experiencing only a static magnetic field $\vec{H}_0$ is the simplest. This gives $\omega(\tau) = \omega_0$ and hence $g(t) = \exp(i\omega_0 t)$. (In practice only $\cos \int_0^t \omega(\tau)\, d\tau$

is usually computed, and the decay is made to refer to a frame rotating at frequency ω_0 so the absorption signal appears at zero frequency.) This elementary fixed-frequency case is easily extended to treat the static dipolar powder spectrum[23] for a sample of randomly oriented pairs of spins. Here the resonance frequency for a given orientation of a pair is given by

$$\omega = \pm \alpha (3 \cos^2 \theta - 1) \tag{2}$$

where $\alpha = 3 \mu^2/\hbar r^3$, and θ is the angle between $\vec{H}_0$ and the pair internuclear vector $\vec{r}$. μ denotes the magnetic moment for the spin. The dipolar powder spectrum which results from summing the set of frequencies over all possible pair orientations is shown in Fig. 1a.

Another simple case, whose features suggest the fundamental issue in motional narrowing, treats a small local field H' jumping randomly between the values $+|H'|$ and $-|H'|$ at a rate $1/\tau_c$. If γ is the magnetogyric ratio for the spin species, then, in the rotating frame,

$$\omega(\tau) = \gamma H'(\tau) \tag{3}$$

and one can show from simple averaging arguments that

$$\int_0^t \omega(\tau)\, d\tau \sim \gamma |H'| \sqrt{t \cdot \tau_c} \tag{4}$$

for a typical series in $\omega(\tau)$. The decay $g(t)$ proceeds to $1/e$ of its initial value as this integral goes to 1 (indicating a mean

FIGURE 1

Dipolar powder spectra. (A) nmr spectrum of isolated pairs of spins in a rigid lattice; and (B) nmr spectrum of isolated equilateral triangles of spins, when the triangles are allowed rapid reorientation about their three-fold symmetry axis (the "methyl rotor" powder spectrum).

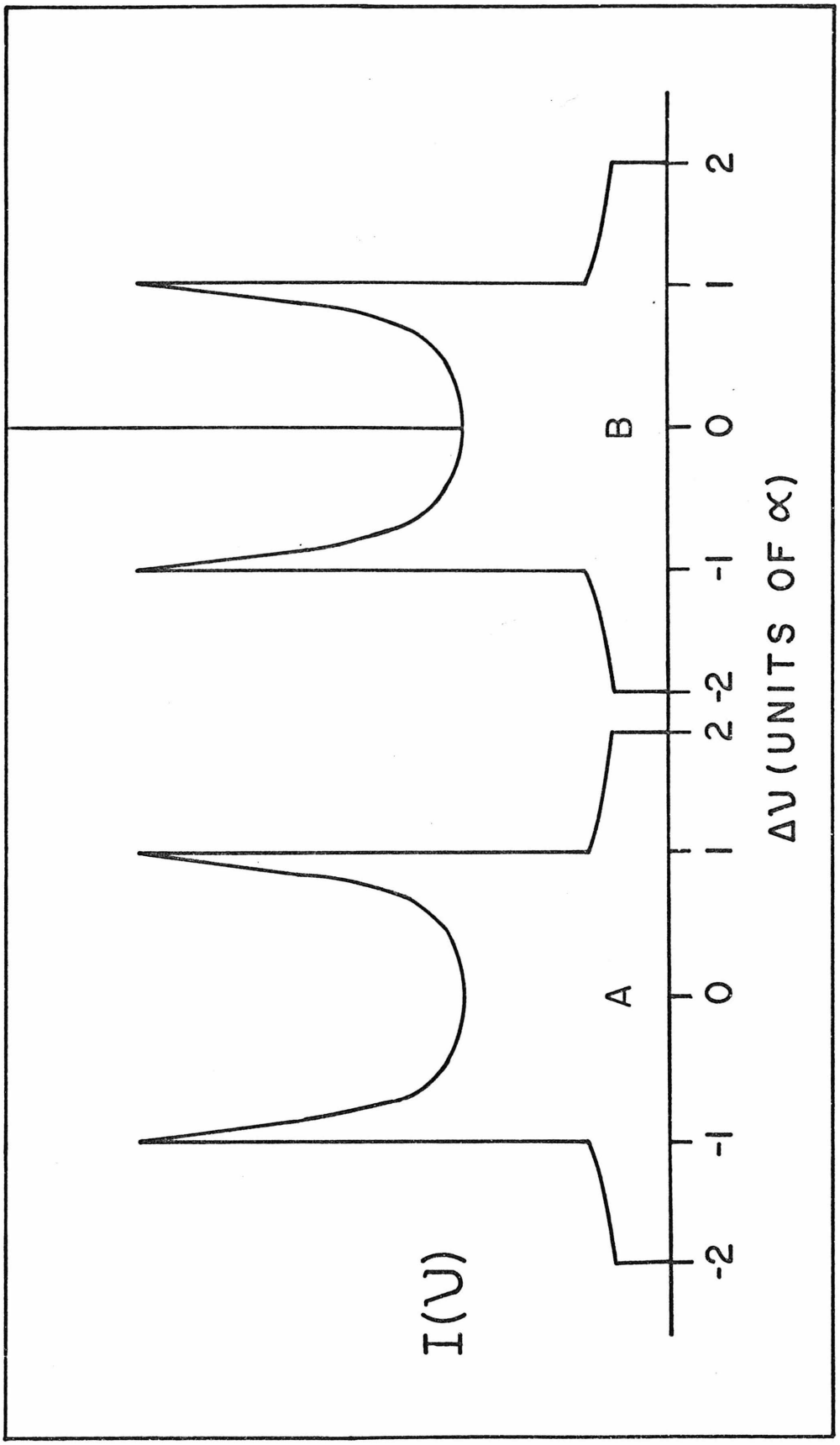
I(ν)
A
B
-2
-1
0
1
2
-2
-1
0
1
2
Δν (UNITS OF α)

dephasing of 1 radian). The time constant for this decay thus has the value

$$\frac{1}{T_2} \cong \gamma^2 \left| H' \right|^2 \cdot \tau_c \qquad (5)$$

The next level of application is to the problem of motional averaging of dipolar broadening, a case which has been treated both analytically (Fixman)[24] and numerically (Saunders and Johnson).[20] The dipolar field is still represented by Eq. (2), but $\theta(\tau)$ and hence $\omega(\tau)$ are now made time-dependent by molecular reorientation, and the internuclear vector $\vec{r}$ described above is allowed to reorient randomly inside a sphere. The distribution of directions of $\vec{r}$ can be found by solving a diffusion equation or by actual dynamical simulation of the motion. The second procedure gives values of $\theta(\tau)$ and hence $\omega(\tau)$ directly after each step, and the integral $\int_0^t \omega(\tau)\, d\tau$ just becomes a sum. As would be expected, when the reorientation rate of $\vec{r}$ becomes fast compared to $1/\alpha$, the dipolar pattern collapses to a single Lorentzian line.

Extension to Restricted Motions

The extension of the procedure of Saunders and Johnson to the motional narrowing observed in pmr spectra of bilayers requires the introduction of constraints on the motion of the internuclear vectors. These constraints are designed to simulate a condition of restricted motion, a state which must be distinguished

from the usual motional states in high resolution nmr. The most frequently encountered states there are simply isotropic and anisotropic. Isotropic describes motion which is unrestricted in space and can be characterized by a single motional correlation time τ_c. Anisotropic motion occurs when a body is still tumbling freely, but has different rates of reorientation about different principal axes, e.g., both $\tau_\perp$ and $\tau_\parallel$ are needed to specify the motions of a cigar-shaped body.

Restricted motion occurs when a body is no longer tumbling perfectly freely in space. This situation can have two origins. First, a cigar-shaped body could be confined, perhaps, in a loose-fitting cylinder, and its long axis could be free to cover only a small range of angles with respect to the cylinder direction. Second, a body could have a net statistical orientation, as in nematic liquid crystals or molecules oriented by applied electric fields. In both of these cases, the intramolecular dipolar fields will not be averaged to zero.

The average intramolecular dipolar field produced by each of these types of motion may be obtained either from a time average or a statistical average. The time average of these fluctuating fields

$$\overline{H'} \sim \langle 3 \cos^2 \theta(t) - 1 \rangle_{ave} \qquad (6)$$

can be replaced, for times long compared to 10^{-4} sec (the inverse of the dipolar linewidth in frequency units), by the statistical expression

$$\overline{H'} \sim \int_{\varphi_1}^{\varphi_2} \int_{\theta_1}^{\theta_2} (3 \cos^2 \theta - 1)\, P(\theta, \varphi) \sin \theta \, d\theta \, d\varphi \ . \qquad (7)$$

Here $P(\theta, \varphi)$ is a statistical weighting function which accounts for the equilibrium distribution of directions that can be assumed by the direction of $\vec{r}$, the internuclear vector.

For the case of isotropic motion, the domain of integration is the surface of the unit sphere (i.e., $\theta \rightarrow [0, \pi]$, $\varphi \rightarrow [0, 2\pi]$) and $P(\theta, \varphi)$ is constant, so $\overline{H'} = 0$. The distribution function P being constant means that all directions in space are equally likely for $\vec{r}$ after long times. Anisotropic motion as defined above satisfies the same conditions, differing from the isotropic case only in the rate at which $\overline{H'}$ approaches zero.

The case of restricted motion introduces the possibility of average fields $\overline{H'}$ not equal to zero. For example, a net statistical orientation of a molecule by an external electric field will produce a $P(\theta, \varphi)$ which is not constant and will reflect the preferred directions for $\vec{r}$. This will give rise, in general, to average fields $\overline{H'}$ that are non-zero. The restricted motions which are considered in this paper specify distribution functions $P(\theta, \varphi)$ which are essentially rectangular, and restrict the possible orientation directions of $\vec{r}$ to certain patches on the surface of the unit sphere. Since P is zero outside these allowed regions, the average $\overline{H'}$ could be found by restricting the domain of integration.

The angles which are used in this paper to characterize the restricted motion of protons on the lipid chains are described

with reference to Fig. 2. The angle θ between the internuclear vector $\vec{r}$ and the applied magnetic field $\vec{H}_0$ is the angle of physical interest, and it is calculated most conveniently in terms of β (the angle between $\vec{r}$ and the chain direction $\vec{c}$), and θ' (the angle between $\vec{c}$ and $\vec{H}_0$), and φ (the phase angle of $\vec{r}$ about $\vec{c}$ minus the phase angle of $\vec{c}$ about $\vec{H}_0$). The models of proton motion which will be investigated can be described by the amount of fluctuation they allow in β and φ. The value of $(3 \cos^2 \theta - 1)$ is evaluated in terms of β, θ', and φ by the addition theorem for spherical harmonics (see Eq. 32 below).

In the type of motion called Case A, β is allowed to fluctuate over the range $[\bar{\beta} + \Delta\beta, \bar{\beta} - \Delta\beta]$ and φ can fluctuate freely. This model accounts for realistic proton motions, such as trans-gauche bond rotations or kink formation. Another type of motion, called Case B, has the same restriction on β but an additional restriction of φ to a range $[\bar{\varphi} + \Delta\beta, \bar{\varphi} - \Delta\beta]$. This case represents restriction of the motion of pairs around the chain axis $\vec{c}$, a condition which would occur in lipid dispersions below the crystalline $\rightleftharpoons$ liquid crystalline phase transition temperature.

Application

The computer program used here is a simple extension of that of Saunders and Johnson. Instead of allowing the direction of $\vec{r}$ to move over all directions, angular restrictions are imposed on the motion, resulting in the "random walk with reflecting

FIGURE 2

Definition of relevant angles. $\vec{H}_0$ is the direction of the applied magnetic field, $\vec{r}$ is the interproton vector, and $\vec{c}$ is the chain axis direction. The angle between $\vec{r}$ and $\vec{H}_0$ is called θ, the angle between $\vec{c}$ and $\vec{H}_0$ is called θ', and the angle between $\vec{r}$ and $\vec{c}$ is called β. The azimuthal angle φ is the difference between φ_c, the phase angle of the projection of $\vec{c}$ in the x-y plane, measured from y, and φ_r, the phase angle of $\vec{r}$ about $\vec{c}$, again measured from y.

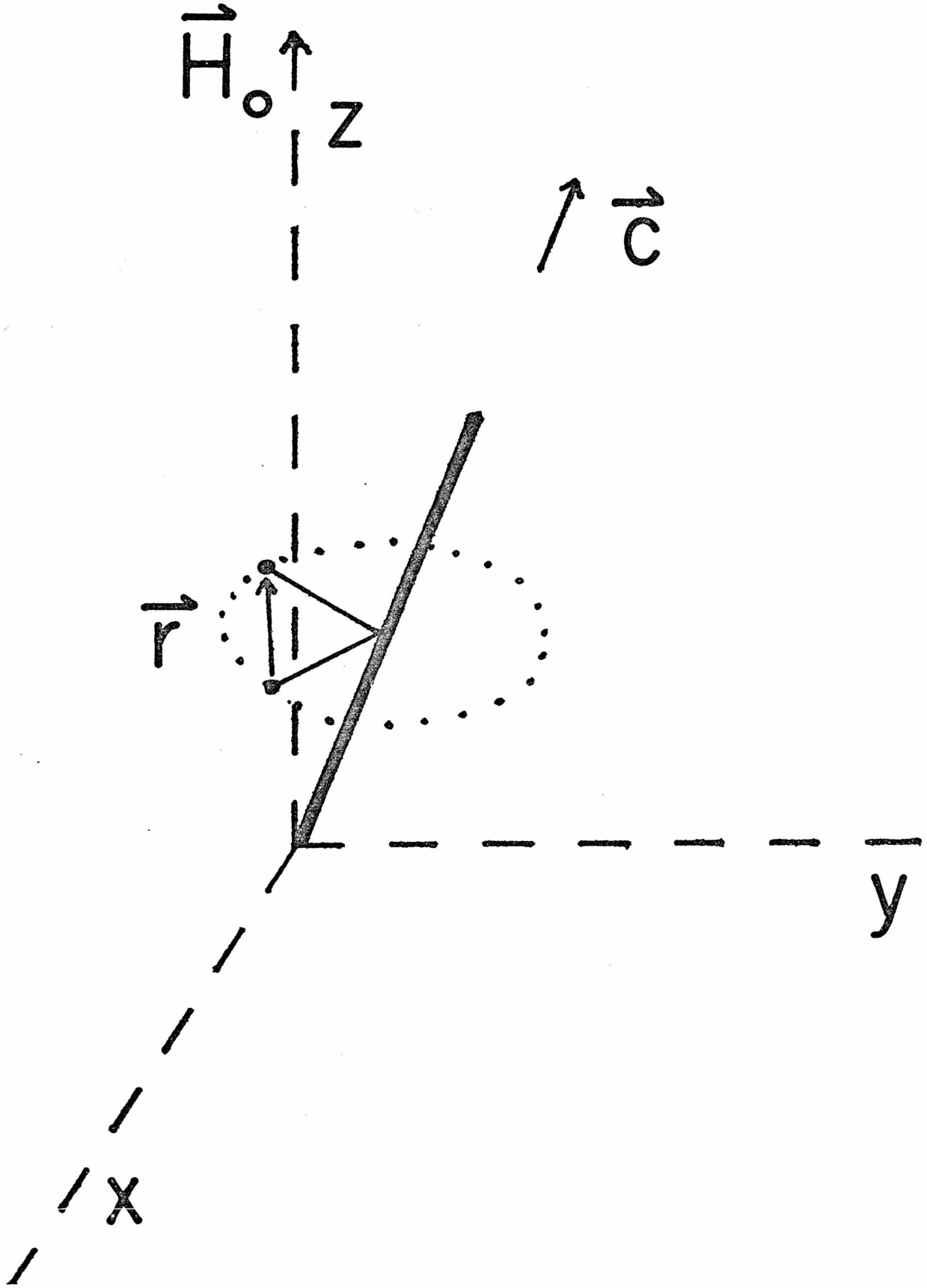
$\vec{H}_o$
z
$\vec{c}$
$\vec{r}$
y
x

barriers" described above. This random walk is generated by the computer program, and g(t) is obtained from the frequency sequences generated by the random walk motion. All motional time scales in the program are defined in terms of $1/\alpha$. For motions like those shown in Case A, it is possible to define two diffusion rates, one in $\Delta\beta$ and one for reorientation in the angle φ. Finally, the g(t) obtained is transformed to frequency space using a fast Fourier transform algorithm.

In this section, results are first obtained for pairs of proton spins on chains undergoing restricted flexing motions. Next, the effects on this pair spectrum of other intramolecular methylene protons will be considered. Finally, spectra will be calculated for methyl group protons. The extension of this program to the calculation of spectra more complex than the two-spin dipolar case is straightforward. The powder spectrum of a methyl group, for example, has several sets of transitions,[25] and these transitions do not all have the same dependence on the orientation angles of the methyl group in the applied magnetic field. If the motion of the group does not make possible new types of transitions, but only perturbs the frequencies of those in the original spectrum, then the parts of the motionally averaged spectrum can be computed independently, following the frequency sequences generated by the motion of the group just as above. The application of this procedure to the methyl pmr spectrum is discussed below in detail.

Pairs of spins. Calculated pmr spectra arising from isolated pairs of spins on chains undergoing various degrees of restricted motion are summarized in Fig. 3. Two sets of simulated spectra are displayed, corresponding to the two types of motional restriction depicted in Fig. 1 (set A corresponds to the motion in Case A, set B to Case B). Lorentzian background broadening has been superimposed on the spectra, 500 Hz in set A and 1000 Hz in set B. The background broadening was deliberately made small so that the two humps characteristic for the dipolar powder spectrum may still be seen. A more realistic broadening, accounting for neighbor protons outside the pair, would be comparable in magnitude to $\Delta\nu_{eff}$, the hump-to-hump splitting. The spectrum would then consist of a simple hump of width $\sim \Delta\nu_{eff}$ at half-height.

The motional correlation times used in the calculations were $\tau_\perp = 1/5\ \alpha$ (sec) for motion in $\Delta\beta$ and $\tau_\parallel = 1/10\ \alpha$ for reorientation about $\vec{c}$. Values of $\tau_\perp$ faster than this produced no significant further averaging. In cases of restricted motion, the overall spectral width will depend only on the degree of restriction, as long as $\tau_\perp$ and $\tau_\parallel$ are sufficiently fast. The actual values of these correlation times must be determined from additional experiments, e.g., magic-angle orientation, Waugh multi-pulse dipolar narrowing studies, and T_1 measurements. Very slow correlation times ($\tau_\perp \geq 1/\alpha$) give no narrowing at all. This is a simple consequence of the fundamental principle in motion

narrowing, i.e., that to be effective in narrowing, a motion must cause fluctuations in the local fields which are fast compared to the inverse of the width of the frequency distribution these fields produce in the static case.

The motion of pairs about the $\vec{c}$ axis can be shown to reduce the effective width of the spectrum by one-half. When the motion in φ is simulated directly, the spectra which result are essentially the same as those generated by replacing α by $\alpha/2$. Spectra obtained with this scaling factor are shown in Fig. 3A. Since the exact shape of the free induction decay is more sensitive to the averaging method than these frequency spectra are, only free induction decays calculated by direct simulation are used for direct comparison with experiment (see below). The basis of the scaling effect used in Fig. 3A is the average relationship

$$\overline{3\cos^2\theta - 1} = (3\cos^2\theta' - 1) \cdot \tfrac{1}{2}\,\overline{(3\cos^2\beta - 1)}\,, \qquad (8)$$

which is true for rapid motions in φ (see Eq. 32). When the appropriate ensemble average over values of θ' is taken, the two "bumps" of the powder pattern are expected to shift in towards the origin by $\sim 50\%$ as compared to the case with restricted motion in φ.

The implications of this simple model are made clear by a comparison of calculated and experimental free induction decays. The experimental effective T_2 for all the protons in a sample of egg lecithin bilayers,[11] for example, is $\sim 120\ \mu$sec. This

FIGURE 3

Dipolar powder spectra for isolated pairs of spins undergoing varying degrees of restricted motions of amplitude $\Delta\beta$, for two types of motion. Case A allows the spins reorientation about a $\vec{c}$ axis (Fig. 2) and case B does not.

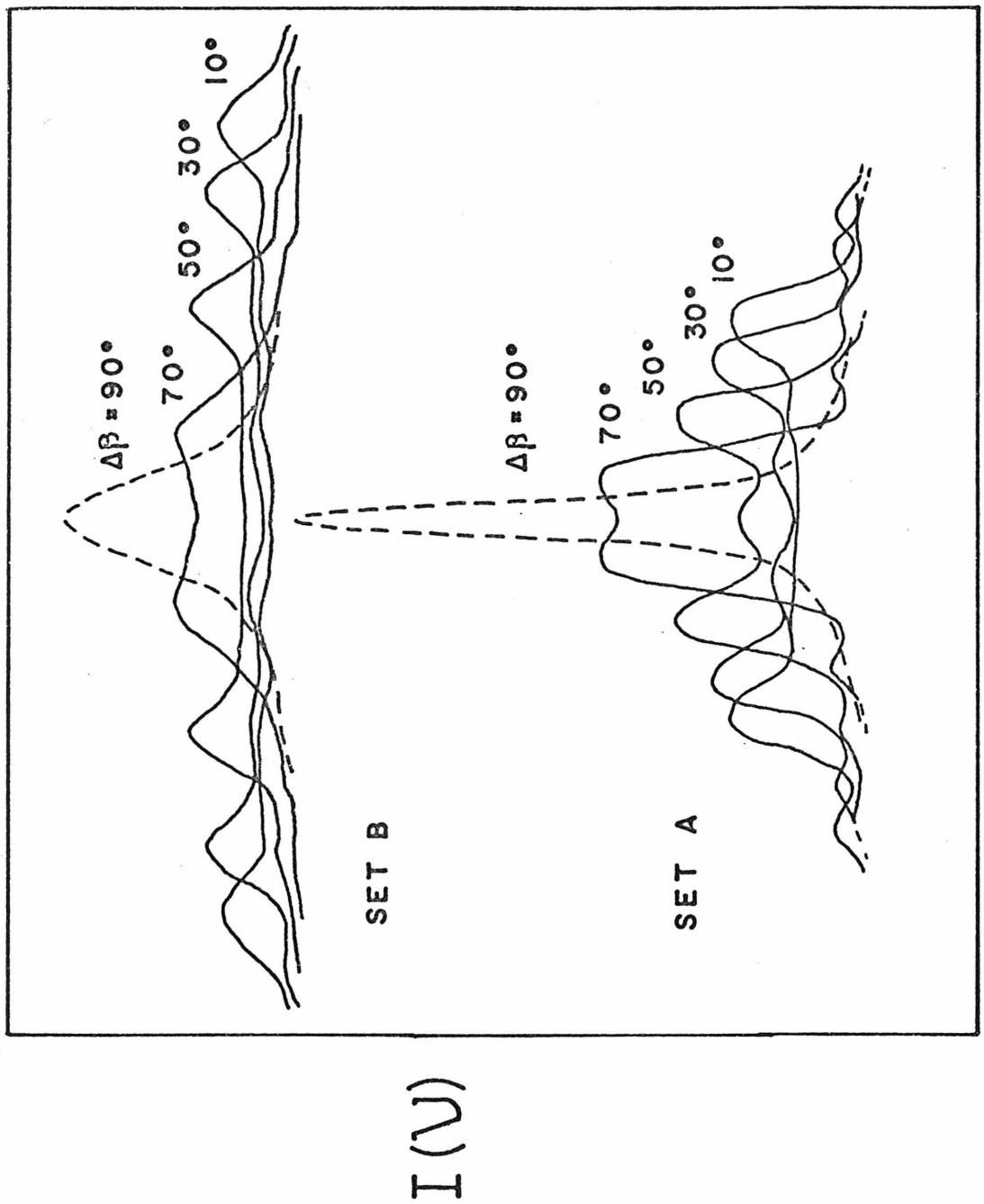
Δβ = 90°
70°
50°
30°
10°
SET B
SET A
-16
-12
-8
-4
0
4
8
12
16
I(ν)
Δν (Hz x 10⁻³)

effective T_2 is the time at which the free induction decay has diminished to 1/e of its original value. What this relaxation time corresponds to in terms of local motions may be estimated from Table I. This table lists the effective T_2's calculated for proton pairs undergoing various degrees of restricted motion, of both the types considered in this paper. As can be seen at once, the case in which proton pairs can reorient about their $\vec{c}$ (chain) axis and execute fairly large ($\Delta\beta \sim 60°$) flexing motions most closely approximates the case of protons on lipid chains in bilayers. Since the greatest broadening influence on a given chain proton is the influence of its pair-neighbor attached to the same carbon, the simple model of moving pairs gives a reasonably accurate representation of the motional narrowing situation for protons on lipid chains in bilayers.

The experimental free induction decay from protons in bilayers is compared with several calculated free induction decays for proton pairs undergoing restricted motions in Fig. 4. Here the solid line is the first part of a reported[11] free induction decay from the protons in egg lecithin bilayers, and the dashed lines are calculated free induction decays for different amplitudes $\Delta\beta$ of restricted motion of type A (which includes motion about chain axis). The first part of the experimental decay is taken because it represents mostly the free induction decay arising from the fast-relaxing methylene protons of the hydrocarbon chains in the bilayers, while the later parts of the free induction

TABLE I

Effective T_2's for proton pairs undergoing various degrees of restricted motion

Case A		Case B	
$\Delta\beta$	$T_{2\,eff}$ (μsec)	$\Delta\beta$	$T_{2\,eff}$ (μsec)
10°	32	10°	14
30°	38	30°	18
50°	70	50°	25
60°	100	60°	45
70°	180	70°	72
90°	260		

Case A and Case B refer to the motional situations described in the text.

FIGURE 4

Calculated and experimental free induction decays. The experimental curve is the first part of the free induction decay from egg lecithin bilayers (see reference 11 of text). The calculated free induction decays arise from pairs of spins undergoing different amplitudes of restricted motion but unhindered reorientation about a $\vec{c}$ axis (Fig. 2).

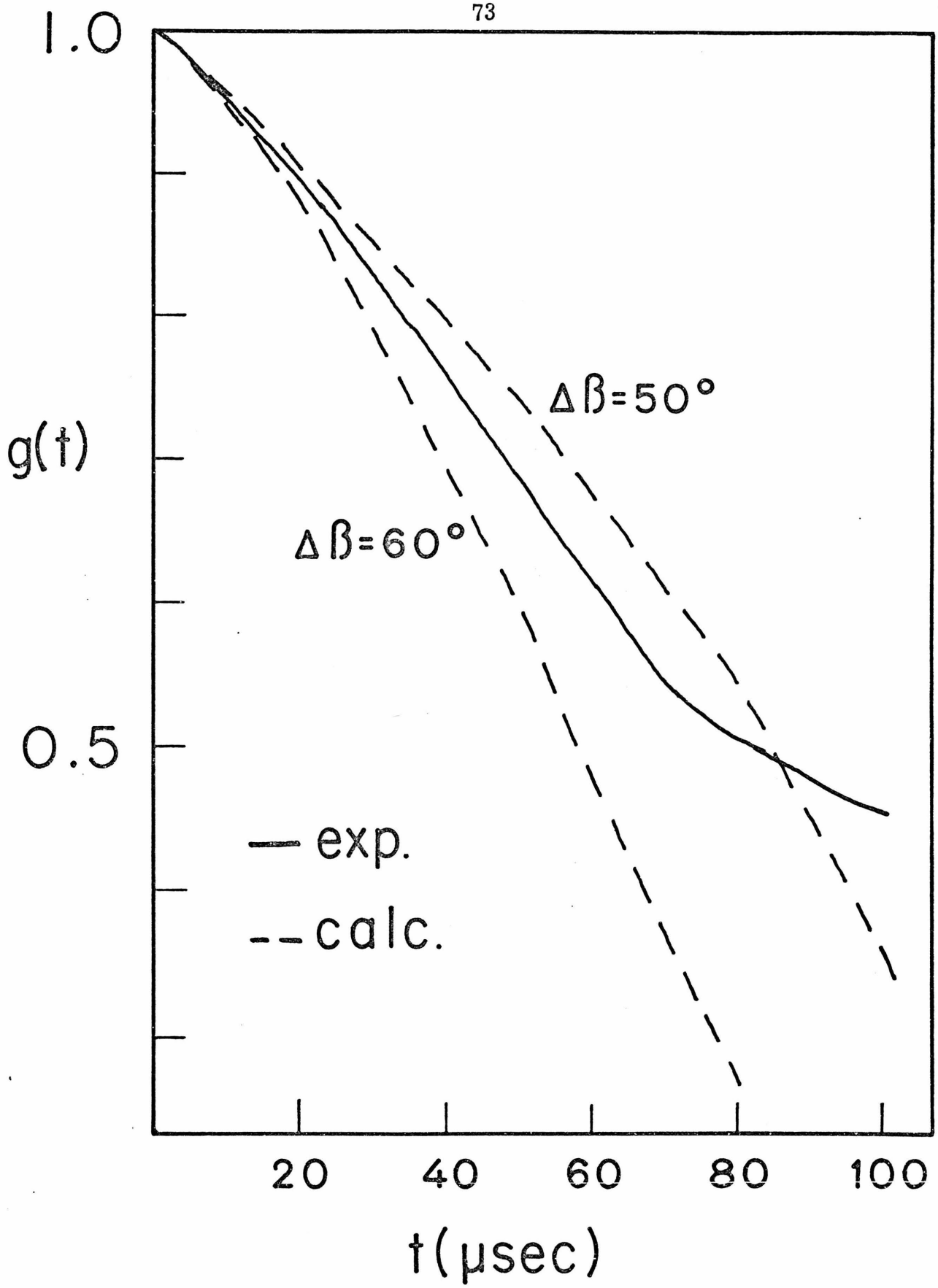
1.0
0.5
g(t)
Δß=50°
Δß=60°
— exp.
-- calc.
20
40
60
80
100
t(μsec)

decay originate from the sharper methyl resonances. This plot shows that the free induction decay of these methylene protons strongly resembles that arising from pairs of spins undergoing restricted motions of amplitude $\Delta\beta \sim 60°$ while reorientating about a $\vec{c}$ axis.

Methylene chain protons. The results from the simple two-spin patterns suggested calculation for chain protons that allowed reorientation about $\vec{c}$ the chain axis and motion in $\Delta\beta$ of amplitude $\sim 60°$. An attempt, however, must be made to include the effects of other protons on the chain as a more realistic model than the simple pair of spins. These other protons of the chain contribute a field at proton 1 of the pair which may be expressed in frequency units as

$$\omega' = \tfrac{3}{4}\ \gamma^2 \hbar \sum_j (3\cos^2\theta_{1j} - 1)/r_{1j}^3 \qquad (9)$$

where the symbols have their usual interpretation. This expression is just the sum of the dipolar fields from individual protons. Since these fields are small[27] compared to that which produces the pair splitting, accounting for ω' in this way is as valid as solving for the splittings of the coupled n-spin system in terms of the angles θ_{1j}. If the protons reorient about the $\vec{c}$ axis, Eq. (9) may be rewritten as

$$\omega' = \tfrac{3}{4}\gamma^2\hbar \cdot \tfrac{1}{2}(1 - 3\cos^2\theta')\ \sum_j \left[(3\cos^2\gamma_{1j} - 1)/r_{1j}^3\right] \qquad (10)$$

where θ' is the angle between $\vec{c}$ and $\vec{H}_0$ and γ_{1j} is the angle

between $\vec{c}$ and a vector joining protons 1 and j.

This transformation is just a special case of the addition theorem for spherical harmonics, and is analogous to the substitution (Eq. 8) performed earlier for reorientation about $\vec{c}$. The relation

$$\omega_T = \tfrac{1}{2} \cdot (1 - 3\cos^2\theta') \cdot [\alpha \cdot (3\cos^2\beta - 1) + \alpha' \sum_j (3\cos^2\gamma_{1j} - 1)/r_{1j}^3] \quad (11)$$

thus is sufficient for finding the g(t) for a typical chain proton, including the broadening effects of chain neighbor protons. Appropriate restricted random walks are generated in β and the γ_{1j}'s, and a background broadening, small in terms of α, can be added as an intermolecular contribution.

Results of such a calculation, which allowed $\Delta\beta = 60°$, an effective $\Delta\gamma = 30°$, and 100 Hz Lorentzian intermolecular background broadening as an upper limit to the intermolecular contribution is shown in Fig. 5. The sharp line in the center refers to a sample in which $\vec{c}$ axes are oriented at 54° to $\vec{H}_0$, close to the magic angle. More pronounced magic angle effects are possible with orientation at 54°44' but the very long g(t) which results is rather expensive to compute. The principal effect of including these other chain protons in the calculation can be seen as a smoothing of the original features of the two-spin spectrum and an additional slight broadening (~ 10% increase in linewidth). Thus the two-spin dipolar spectra are a good approximation to the spectra of chain protons in bilayers.

FIGURE 5

Motionally averaged dipolar spectra of methylene chain protons, including effects of intra-chain neighbors. These protons are assumed to undergo restricted motion of type A with amplitude $\Delta\beta$ = 60°. The dashed line is the spectrum arising from a randomly oriented collection of such chains, while the solid line is the spectrum arising from a collection of chains whose $\vec{c}$ axes are oriented at the "magic angle", θ' = 54°44' to the applied field $\vec{H}_0$.

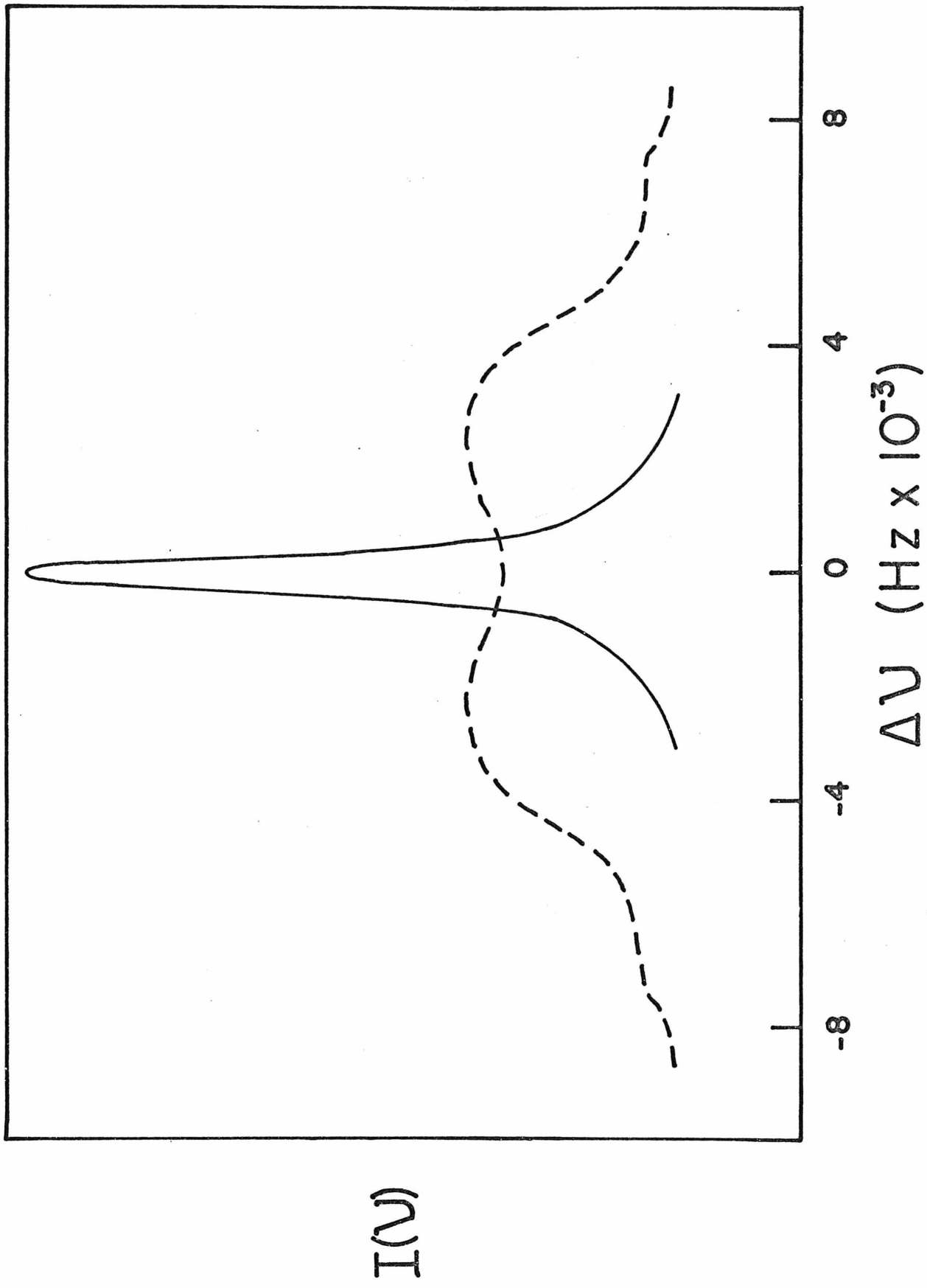
I(ν)
-8
-4
0
4
8
Δν (Hz x 10⁻³)

An estimate of the intermolecular broadening contribution[8] used above for unsonicated bilayers can be obtained from the treatment of Kruger.[28] This investigator has given a procedure for estimating the contribution of intermolecular dipole-dipole interactions to the linewidth and spin-lattice relaxation if this interaction is modulated by translational diffusion. In this particular case, lateral diffusion of lipid molecules causes the intermolecular dipolar fields at a given proton to fluctuate as the lipid chains exchange positions. Since chain protons may have $S_z = +\frac{1}{2}$ or $S_z = -\frac{1}{2}$ with essentially equal probability, this position exchange among chains causes a proton to experience intermolecular fields fluctuating at a rate τ_{ex}, the chain position interchange time, which can be related to the lateral diffusion constant D. In phospholipid bilayers, D has been determined experimentally,[29] and found to be 2×10^{-8} cm^2/sec. This diffusion rate, when used in the theory of Kruger, gives a linewidth estimate of ~ 20 Hz, essentially independent of the detailed diffusion model. This prediction also agrees with the oriented-bilayer experiment of De Vries,[15] which demands that intermolecular broadening be less than ~ 100 Hz.

Methyl protons. The powder spectrum of isolated rotating triangles of spins given by Andrew and Bersohn[30] is the starting point for calculations[31] of the restricted motional spectra of methyl protons. The spin Hamiltonian for an equilateral triangle of spins may be written as

$$\mathcal{H}' = -\gamma\hbar H_0 \sum_{i=1}^{3} I_{z_i} + \sum_{i>j} (\vec{I}_i \cdot \vec{I}_j - 3 I_{z_i} I_{z_j}) A_{ij} \qquad (12)$$

where

$$A_{ij} = \frac{\gamma^2 \hbar^2}{2 r^3} \cdot (3 \cos^2 \theta_{ij} - 1) \qquad (13)$$

The substitution $\cos \theta_{ij} = \cos \theta'_m \cos \beta + \sin \theta'_m \sin \beta \cos \varphi_{ij}$ can be used in Eq. (13) to show that rapid rotation of the three-spin group about its C_3 symmetry axis averages all the A_{ij}'s to the same value. Here θ'_m is the angle between the C_3 axis and the applied magnetic field $\vec{H}_0$, and $\beta_m = 90°$ is the angle between the $\vec{r}_{ij}$ and the C_3 axis. The average Hamiltonian then gives rise to a set of transitions at frequencies $-4x'$, 0, and $+4x'$, with intensity ratios of 1:2:1. Here x' has the value

$$x' = \frac{1}{4} (\bar{A}_{12} + \bar{A}_{23} + \bar{A}_{13}) \qquad (14a)$$

$$= \frac{3}{16} \frac{\gamma^2 \hbar^2}{r^3} (1 - 3 \cos^2 \theta'_m) \qquad (14b)$$

The powder spectrum resulting from this set of transitions is shown in Fig. 1b. This spectrum, characteristic of isolated rotating triangles of spins, has two main features: broad dipolar wings containing 50% of the spectral intensity, and a sharp central spike containing the rest of the intensity.

If these isolated rotating triangles are now allowed to undergo restricted motions of their C_3 axes, the dipolar wings of the spectrum will be motionally narrowed in the same way as a two-spin spectrum under the analogous restricted motion, but

the central spike, whose frequency is angle-independent, will still have zero width. Thus the width of this central methyl resonance (~ 200 Hz, as observed in delayed Fourier transform (FT) experiments of lecithin bilayers[21]) arises because the spins of the methyl triangles are not isolated but have neighboring spins, e.g., methylene protons or other methyl groups. The linewidth of the methyl center spike, which is the resonance observed in delayed FT experiments (the dipolar wings being too broad), must be analyzed in terms of these "outside" dipolar fields, or specifically the average of these fields that the methyl protons experience as their C_3 axis undergoes restricted motions.

The outside dipolar fields are usually small compared to the splitting ($|4x'|$) produced by the spins in the methyl group. Furthermore, the closest protons to the triangle (e.g., chain-CH_2 protons next to terminal methyls or methyl neighbors on a choline group) are rigidly connected to the C_3 axis of the methyl (a C-C or C-N bond). These outside fields can thus be described in terms of their angular dependence on θ'_m, and the methyl spectrum can be calculated in exactly the same way as the chain proton spectrum of the previous section.

This procedure must be justified by showing that the center line, the main feature of interest in the methyl spectrum (ordinarily the broad wings will be lost in the methylene signal), behaves under the perturbation of the outside spin as if it arose from the single transition of a one-spin system. The average

Hamiltonian appropriate to this problem is

$$\mathcal{H}'' = \overline{\mathcal{H}'} - \gamma\hbar H_0 I_{z_{ex}} + \sum_{i=1}^{3} (\vec{I}_{ex} \cdot \vec{I}_i - 3 I_{z_{ex}} \cdot I_{z_i}) \overline{A_{ex\,i}} \qquad (15)$$

where the subscript ex denotes the outside spin, and the bar denotes averaging with respect to the three moving spins in the methyl group. When applied to the spin functions listed in Table II for the four-spin problem, this Hamiltonian produces in the center of the spectrum a pair of lines at $\pm 4/3\,x''$ and satellites of negligible intensity at $\pm 4\,x''$ and $\pm 2/3\,x''$, where $x'' = \frac{1}{4}\sum_{i=1}^{3} \overline{A_{ex\,i}}$. Thus the outside spin effectively splits the rotating methyl group center line into two lines, and the value of this splitting, for cases of physical interest, is both small and dependent on the parameter θ'_m. The motional averaging produced in the broad part of the spectrum by fluctuations in θ'_m is accompanied by averaging of this narrow part for the same reasons. The approximation made in regarding the outside spin as producing a simple fluctuating dipolar field is therefore justified, and the "scaling in" of the spectrum in the presence of motion which results from these conditions is clearly seen in Fig. 6.

The dashed line in this figure is the calculated pmr spectrum for methyl groups experiencing rapid rotation about their C_3 axes and undergoing restricted motions in this axis, of amplitude $\Delta\theta'_m = 10°$. These methyl groups also experience a dipolar field from "outside" protons of ~ 0.5 Gauss, a value typical for the field of neighbor methylene protons at the average position of

TABLE II

Spin functions for the special four-spin group[a]

$$\psi_1 = \alpha_{ex}\,\alpha\alpha\alpha \qquad \psi_5 = \beta_{ex}(\alpha\alpha\beta + \alpha\beta\alpha + \beta\alpha\alpha)\,1/\sqrt{3}$$

$$\psi_2 = \alpha_{ex}(\alpha\alpha\beta + \alpha\beta\alpha + \beta\alpha\alpha)\,1/\sqrt{3} \qquad \psi_6 = \alpha_{ex}(\beta\beta\beta)$$

$$\psi_3 = \beta_{ex}(\alpha\alpha\alpha) \qquad \psi_7 = \beta_{ex}(\beta\beta\alpha + \beta\alpha\beta + \alpha\beta\beta)\,1/\sqrt{3}$$

$$\psi_4 = \alpha_{ex}(\alpha\beta\beta + \beta\alpha\beta + \beta\beta\alpha)\,1/\sqrt{3} \qquad \psi_8 = \beta_{ex}(\beta\beta\beta)$$

$$\psi_9 = \alpha_{ex}(\alpha\alpha\beta - \alpha\beta\alpha)\,1/\sqrt{2}$$

$$\psi_{10} = \alpha_{ex}(\beta\beta\alpha - \beta\alpha\beta)\,1/\sqrt{2}$$

$$\psi_{11} = \beta_{ex}(\alpha\alpha\beta - \alpha\beta\alpha)\,1/\sqrt{2}$$

$$\psi_{12} = \beta_{ex}(\beta\beta\alpha - \beta\alpha\beta)\,1/\sqrt{2}$$

[a] The subscript ex denotes the outside spin, mentioned in the text, which is distinguishable from the three spins of the methyl top.

FIGURE 6

PMR spectra of "methyl rotors". The dashed line is the spectrum of rapidly reorienting methyl tops whose C_3 axes are allowed to perform restricted motions of amplitude $\Delta\theta'_m = 10°$. The spectrum includes the effects of neighbor protons to the 3-spin group. The solid line is the spectrum of the same methyls, except that $\Delta\theta'_m$ is now taken as 70°. The vertical bars next to the resultant motionally narrowed methyl center spike represent the effective width of the delayed Fourier transform "window", that is, the maximum width of the resonance lines which can be observed in a typical delayed FT experiment.

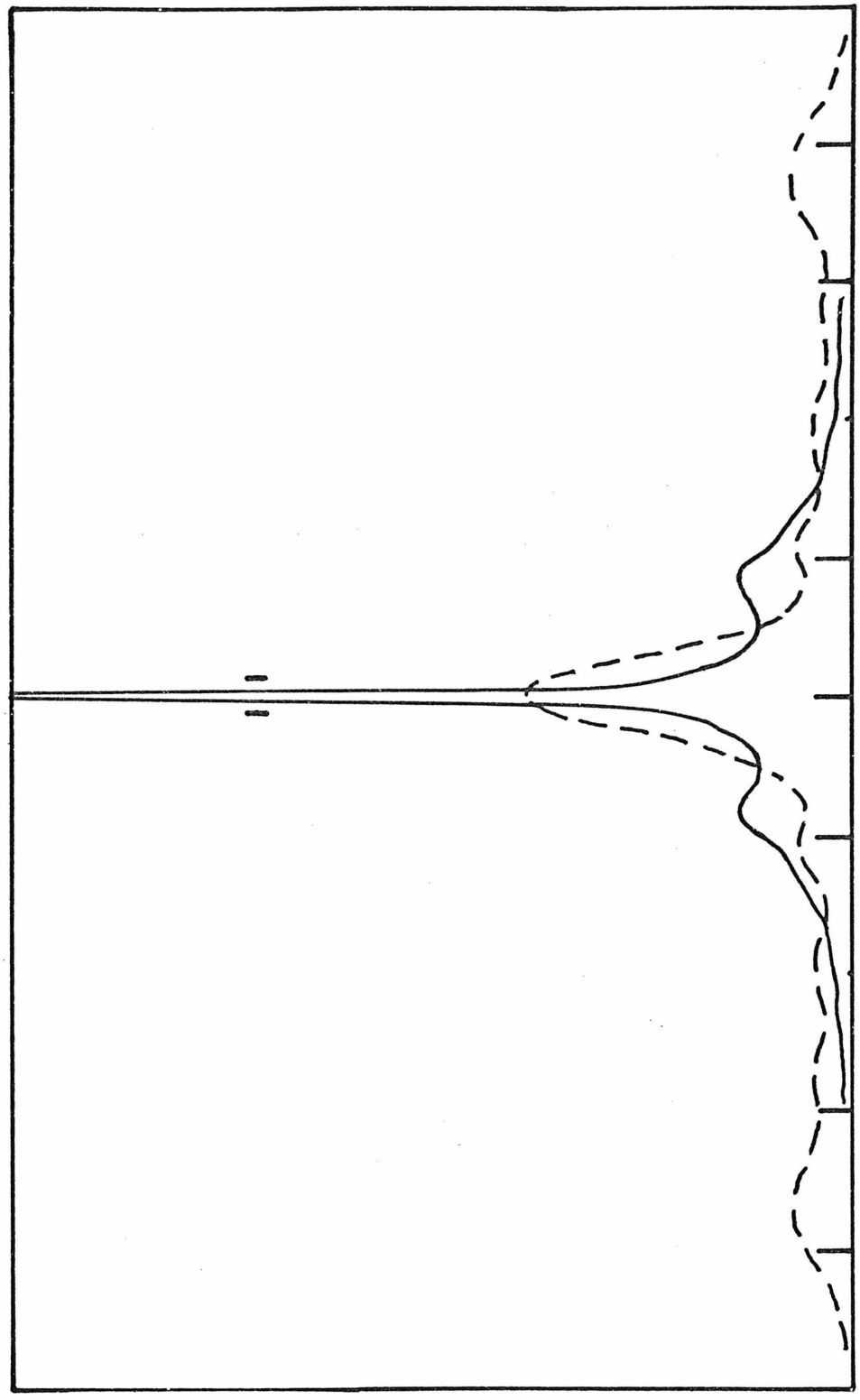
I(ν)
-16
-12
-8
-4
0
4
8
12
16
Δν (Hz x 10⁻³)

the methyl protons. The solid line in the figure depicts the spectrum of these methyl groups under the same conditions of internal rotation and neighbor proton fields, but now the amplitude of restricted motion of the C_3 axes is $\Delta\theta'_m = 70°$. As can be seen, the center peak of the spectrum has a width of a few hundred Hz, comparable to the experimental linewidths of 150-200 Hz observed for both choline and chain terminal methyl protons in lecithin bilayers.[21] The short vertical bars next to this peak in the figure represent the approximate width of the delayed Fourier transform (FT) "window", that is, the part of the spectrum (in this case the methyl center peaks) which is not filtered out by the acquisition delay in the delayed Fourier transform experiments.[21] Thus most of the methyl center peak from a methyl group undergoing restricted motions of amplitude $\Delta\theta'_m = 70°$ should appear in a delayed FT spectrum, with a width of $\sim$ 200 Hz, and this calculation agrees well with the observed data.

This situation is not unusual and has been observed in several different types of magnetic resonance spectroscopy as well. Hubbell and McConnell[32] have analyzed partially averaged hyperfine splittings in esr spectra of spin labels incorporated into bilayer systems. These effects arise because a term in the esr spin Hamiltonian, which is the analog of the dipolar term above, cannot be completely averaged by the motions of the spin label. Shporer and Civan[33, 34] have also reported nuclear quadrupole resonance (nqr) spectra, from ^{23}Na in sodium linoleate bilayers

and $H_2{}^{17}O$ in frog muscle, which show partially averaged quadrupole splittings. The situation in these nqr spectra is analogous to that in the methyl group pmr spectra considered here. In both cases, an apparent intensity anomaly arises because solid-like splittings, too large to be observed except on wide-line spectrometers, leave a central peak of much less than 100% intensity.

Discussion

Implication for bilayers. A motional model of lipid bilayers, which takes into account both chain motions and the motion of polar head groups (e.g., choline in the case of lecithin) can now be brought forth from these calculated spectra. This presentation must start with a review of the experimental pmr linewidth information which the model must be able to explain. Such information is of two distinct types, that referring to chain protons and that referring to the special case of methyl protons.

The protons of lipid chains in bilayers have a pmr linewidth, in the usual case, of 3000 Hz, the range of possible linewidths covering 2500 Hz to 5000 Hz. The linewidth can be shown[11, 14] to be independent of the applied magnetic field. Furthermore, the linewidth of an oriented bilayer sample depends on the angle of the lipid chains to the applied magnetic field.[15, 18]

The protons of chain terminal methyl groups in bilayers, and the protons of the choline head group in lecithin bilayers, show pmr spectra in which peaks of width ~ 100-200 Hz are

found to contain much less than 100% of the signal intensity expected from the concentration of the protons in the sample. The usual intensity for both types of methyl proton is near 50% , but the intensity of the chain terminal proton signal can be made to increase somewhat with temperature.[21]

One immediate conclusion from these data is that the motion of methyl groups on the choline moiety of lecithin in bilayers is seriously restricted, and that a spectrum of the type shown in Fig. 6 is observed from these choline methyl protons. This conclusion is quite straightforward, as it is generally believed that the surface of the bilayer is rigid because of strong charged-group interactions.

A more important conclusion, however, is that the interior of the bilayer has a significant degree of order. A model of motion in which chain protons undergo rapid motion around the chain axis while performing restricted off-axis flexing motions ($\Delta\beta \sim 60°$) accounts for the observed pmr linewidth of unsonicated bilayers and the variation of this linewidth in sample orientation experiments. This motional model, here described chiefly in terms of degree of motional restriction, may be compared to conventional physical models of chain motion, and it is possible to decide which of these models, e. g. trans-gauche rotations,[35] gauche$^+$ gauche$^-$ rotation pairs,[35, 36] or kink formation,[37] this current picture most closely resembles.

Trans-gauche rotations occur about a single bond and bend

the hydrocarbon chain at the point of rotation. Thus, although this mode provides the desired motion for a given proton pair, it would not maintain a sufficient degree of motional restriction for chain terminal methyl groups, as numerous bends in the chain would allow segments near the end to take an almost random orientation. Trans-gauche rotations are therefore not a good description of the flexing of chains in unsonicated bilayers.

Gauche$^+$ gauche$^-$ rotations or kink formation, which are essentially equivalent operations on a hydrocarbon chain, allow suitable motion for individual proton pairs and also maintain segment-wise chain orientation. Because this mode of motion does not swing chain sections out of their orientation perpendicular to the bilayer surface, it permits the chains to stay in a relatively solid-like packing. This feature, the maintenance of packing order, is important because it implies that the motion even of the chain terminal methyl groups will be restricted, and thus the characteristic restricted motion spectrum of methyl groups (Fig. 6) would explain the signal intensity anomaly and the narrow linewidth observed in the pmr spectra of these protons. The amplitude of flexing associated with this motion is of the order $\Delta\beta \sim 60°$, as required from linewidth considerations. Furthermore, kink formation on a part of the chain near the ionic head causes rotation of the rest of the chain with no associated local flexing, thus producing the condition $\tau_{\|} < \tau_{\perp}$ for the chain methylene protons. In summary, the motion of chains in unsonicated bilayers

resembles sterically the motion of chains in solid polyethylenes[38] or paraffins, but occurs on a faster timescale.

T_1 interpretation. The motional model derived above from linewidth considerations should also agree with the observed results on spin-lattice relaxation. The most important of these results is the observation that, over a wide range of temperatures and frequencies, the bulk proton spin magnetization recovery in a lipid bilayer proceeds with a single spin-lattice relaxation rate. This result has two main implications. First, the dipole-dipole coupling of the methylene spins must be sufficiently strong that spin-diffusion[39] must be invoked to explain why these methylene protons do not exhibit different T_1's. Spin-diffusion to those spins with efficient thermal relaxation is characteristic of samples with broad resonance linewidths and has been demonstrated to control T_1 in solid and semi-solid hydrocarbons.[36] Second, the methyl protons in the bilayer account for 20% of all the protons in the sample and could introduce non-exponentiality into the bulk magnetization recovery if their T_1 were very different from that of the methylene system. Experimentally, the methyl proton magnetization recovery has been observed[21] separately from the bulk, and is found to be exponential, with a T_1 close but not identical to that of the methylenes.

Analysis of the proton T_1 data from unsonicated lipid bilayers could then be expected to yield motional information about two species of protons: those protons which act as the

"heat sink" for the spin diffusion process and hence determine the T_1 of the methylene system; and the methyl protons, which relax independently of the methylenes. The T_1 process is more sensitive to motions which are more rapid and of smaller amplitude than those motions which determine the restricted-motion linewidth, and the T_1 analysis should supplement and independently confirm the motional results of linewidth analysis.

Motional information about these protons can be obtained from T_1 data using a modification of a formula of Woessner[40] for relaxation by anisotropic motion. This formula is applicable to relaxation of pairs of methylene protons, and is extended to relaxation of methyl groups by assuming an uncorrelated contribution to relaxation from the additional proton.[41, 41] The same result has been obtained in a much more general form by McBrierty and Douglass,[42, 43] but the following specialization is adequate for the bilayer problem, and allows a quantitative discussion of local motions. The evaluation only of the intramolecular contribution to T_1 in this case can be justified by reference to experimentally measured intermolecular T_1 contributions.[8]

The well-known formula

$$\frac{1}{T_1} = \frac{9}{8} \frac{\gamma^4 \hbar^2}{r^6} \{J_1(\omega_0) + J_2(2\omega_0)\} \tag{16}$$

where

$$J_k(\omega) = \int_{-\infty}^{+\infty} e^{i\omega\tau} \cdot \overline{F_k(\tau) F_k(0)}\, d\tau \tag{17}$$

$$F_1(\tau) = \sin\theta(\tau)\cos\theta(\tau) \tag{18}$$

and

$$F_2(\tau) = \sin^2\theta(\tau) \tag{19}$$

can be expanded explicitly for a model of anisotropic motion of a pair of spins such as that illustrated in Fig. 2. That is, motion of the axis $\vec{c}$ occurs on a timescale $\tau_\perp$, and motion of the pair about this $\vec{c}$ axis occurs on a timescale $\tau_\parallel$. In Woessner's formulation β is fixed (here $\beta = 90°$) and θ' is allowed to fluctuate. Motion about the $\vec{c}$ axis occurs on a timescale $\tau_\parallel$, and motion in θ' occurs on a timescale $\tau_\perp$. Because $\beta = 90°$ and free motion around $\vec{c}$ is allowed, the averaging range $\Delta\theta'$ based on Woessner's treatment is exactly equivalent to the range $\Delta\beta$ used in our linewidth calculations. Defining a new correlation time τ_c as

$$\frac{1}{\tau_c} = \frac{1}{\tau_\perp} + \frac{1}{\tau_\parallel} \quad ,$$

Eq. (16) becomes

$$\begin{aligned}\frac{1}{T_1} = \frac{9}{8}\frac{\gamma^4\hbar^2}{r^6}\Bigg\{&\frac{1}{4}\overline{(\sin\theta'\cos\theta')^2}\cdot\frac{2\tau_\perp}{1+\omega_0^2\tau_\perp^2} \\ &+ \frac{1}{8}\overline{\sin^2\theta'(1+\cos^2\theta')}\cdot\frac{2\tau_c}{1+\omega_0^2\tau_c^2} \\ &+ \frac{1}{4}\overline{(\sin^2\theta')^2}\cdot\frac{2\tau_\perp}{1+4\omega_0^2\tau_\perp^2} \\ &+ \frac{1}{8}\overline{(1+6\cos^2\theta'+\cos^4\theta')}\cdot\frac{2\tau_c}{1+4\omega_0^2\tau_c^2}\end{aligned} \tag{20}$$

where the bars denote averaging over the appropriate angular ranges indicated by the restricted motions. This same equation may also be used to calculate the T_1 of methyl protons, using the assumption of independent relaxation contributions among the three protons. The only modifications are that θ' is replaced by θ'_m and the motion characterized by $\tau_{\|}$ takes place about the methyl C_3 axis. The distinctive feature of Eq. (20) is the complex frequency and temperature dependence of T_1 brought about by the introduction of two correlation times. A plot of T_1 vs. temperature will usually have a special "double-minimum" form, since activation energies for the processes producing the two motions will not in general be equal. Likewise, a plot of T_1 vs. frequency at a given temperature will show a broader T_1 minimum region than will a plot based on a single correlation model. These two types of plot will contain sufficient information to determine both $\tau_{\perp}$ and $\tau_{\|}$. Physically, this result comes about because the type of local field fluctuations which are most efficient for spin-lattice relaxation, i.e., those on timescale $1/\omega_0$, may occur in two different ways in this model, and variations of temperature or resonance frequency can determine which mode of motion is more efficient for relaxation under different conditions.

T_1 data from egg lecithin and dimyristoyl lecithin bilayers can be analyzed with Eq. (20) to yield information about $\Delta\theta'$ $(=\Delta\beta)$, $\tau_{\perp}$ and $\tau_{\|}$ for those protons for which sufficient data are available. The details of the calculation[44] will be reported in detail

elsewhere. For the purposes of this paper it is only necessary to summarize the results. First, the condition $\Delta\beta \geq 60°$ is needed to provide an exponential decay, for both the methyl and methylene protons. Second, those protons which act as the heat sink for the methylene system (perhaps those protons near the end of the chains) have the motional timescale $\tau_\perp \sim 10^{-7}$ sec and $\tau_\parallel \sim 10^{-9}$ sec. The methyl protons are found to have essentially the same $\tau_\perp$ but a faster $\tau_\parallel$, on the order of 10^{-10} sec.

The relation of these correlation times to the linewidth results is physically different from their relation to spin-lattice relaxation, and should be clarified. First, as long as $\tau_\perp < 1/\alpha$, there will be significant motional narrowing of the rigid lattice spectrum, but after this condition is fulfilled the linewidth for restricted motion will depend on $\Delta\beta$ more directly than on $\tau_\perp$. Second, the condition $\tau_\perp \gg \tau_\parallel$ reduces the linewidth (for restricted motions again) by a factor of two from what it would be with $\tau_\perp \leq \tau_\parallel$, and the exact value of $\tau_\parallel$ has no further effect on linewidth even though it is quite important in T_1 considerations. Third, the relationship of these correlation times to linewidth is quite different in sonicated vs. unsonicated bilayers, but we postpone discussion of this topic to a later section below.

T_2 interpretation in the limit of rapid spin diffusion. A treatment of T_2 interpretation for methyl spectra analogous to the T_1 theory was presented earlier by the authors[45] and can be seen in the light of present results to apply only to certain special cases.

When there are rapid ($\sim$2000/sec) $\alpha \rightarrow \beta$ spin flips among the chain methylene protons (i.e., a case of fast spin diffusion) the terminal methyl protons experience a rapidly alternating dipolar field produced bytheir neighbor methylene protons. This field is then averaged to zero on a time scale which is fast compared to the inverse of the splitting (called 4/3 x″ in the exact treatment above) it induced in the static case in the center peak of the methyl spectrum. Under these conditions it is appropriate to describe the relaxation of this center peak using a pseudo-Hamiltonian in which $\overline{\mathcal{H}_1(t)} = 0$. Then only fluctuations in local fields, and not average values of these fields, contribute to linewidth, and the equation

$$\frac{1}{T_2} = \frac{9}{8} \frac{\gamma^4 \hbar^2}{r^6} \left\{ \frac{1}{4} J_0(0) + \frac{5}{2} J_1(\omega_0) + \frac{1}{4} J_2(2\omega_0) \right\} \qquad (21)$$

(where $J_0(0)$ is specified by Eq. (17) and the definition $F_0(\tau) = 3\cos^2\theta(\tau) - 1$), can be developed for restricted motions by averaging the angular functions involved in the spectral density functions J_k over the appropriate restricted angular ranges. The results reported in Ref. 45 follow from this simple procedure, except that the calculated intensities reported there are twice as large as they should be because they concern only the center peak and not the whole methyl spectrum.

This physical situation would conceivably occur in samples of mixed phospholipid-cholesterol bilayers. There the cholesterol packing produces considerable additional motional restriction on

the methylene chains, while leaving terminal methyls more freedom than in pure lipid bilayers.

Formal treatment of the narrowing effects of restricted motions. The chief features of motional narrowing by restricted motions may be explained in terms of the density matrix formalism for relaxation.[46] The time-dependent behavior of the density matrix is expressed by the equation

$$\frac{d\rho}{dt} = \overline{-i\,[\mathcal{H}_0 + \mathcal{H}_1(t),\ \rho\,]} \tag{22}$$

where ρ is the density matrix, $\mathcal{H}_0$ represents the static magnetic Hamiltonian arising from the applied magnetic field $\vec{H}_0$, and $\mathcal{H}_1(t)$ denotes the fluctuating intramolecular dipolar field energy modulated by the motions of the spins. The term $\mathcal{H}_1(t)$ can be made to include other forms of magnetic energy, e.g., anisotropic chemical shift interactions or intermolecular dipolar interactions, when these are felt to be important.

The process of deriving useful relaxation expressions from this equation starts with a transformation of ρ and $\mathcal{H}_1(t)$ to the interaction representation to remove the trivial time dependence of ρ on $\mathcal{H}_0$. This transformation, namely,

$$\rho^* = \exp(i\,\mathcal{H}_0\,t) \cdot \rho \cdot \exp(-i\,\mathcal{H}_0\,t) \tag{23}$$

and

$$\mathcal{H}_1^*(t) = \exp(i\,\mathcal{H}_0\,t) \cdot \mathcal{H}_1(t) \cdot \exp(-i\,\mathcal{H}_0) \tag{24}$$

introduces new variables ρ^* and $\mathcal{H}_1^*$, which may simply be

thought of as ρ and $\mathcal{H}_1$ viewed in a "rotating frame" rotating at a frequency $\omega_0 = \mathcal{H}_0/\hbar$. The time-dependent behavior of the density matrix reduces after this transformation to

$$\frac{d\rho^*}{dt} = -i\,\overline{[\mathcal{H}_1^*(t),\ \rho^*]}\quad , \tag{25}$$

which can then be integrated by successive approximation to yield a series expansion for $\rho^*(t)$. An expression for the time derivative of $\rho^*(t)$, accurate to second order, may be obtained by substituting the first order solution for $\rho^*(t)$ into Eq. (25). The result is

$$\frac{d\rho^*}{dt} = -i\,\overline{[\mathcal{H}_1^*(t),\ \rho^*(0)]} - \int_0^t \overline{[\mathcal{H}_1^*(t),\ [\mathcal{H}_1^*(t'),\ \rho^*(0)]]}\,dt'\,. \tag{26}$$

If $\overline{\mathcal{H}_1}$, and hence $\overline{\mathcal{H}_1^*}$, happens to be zero, this equation simplifies to

$$\frac{d\rho^*}{dt} = -\int_0^t \overline{[\mathcal{H}_1^*(t),\ [\mathcal{H}_1^*(t'),\ \rho^*(0)]]}\,dt'\quad , \tag{27}$$

an expression which describes the relaxation of ρ^* in terms of the fluctuations in $\mathcal{H}_1^*(t)$. This result reduces in most cases to familiar expressions for T_1 and T_2, since the terms under the averaging bar are just correlation functions for the appropriate fluctuating fields.

The treatment above, in which $\overline{\mathcal{H}_1} = 0$, applies to the situation of motional narrowing in liquids. However, in the case of restricted motion, the local fluctuating fields do not average to

zero, that is $\overline{\mathcal{H}_1} \neq 0$, and the derivation must be modified. This is done most conveniently by separating $\mathcal{H}_1(t)$ into a constant average part and a time dependent part, as

$$\mathcal{H}_1(t) = \overline{\mathcal{H}_1} + \mathcal{H}_1'(t) \tag{28}$$

and combining $\overline{\mathcal{H}_1}$ with the static Zeeman Hamiltonian $\mathcal{H}_0$. The master equation, rewritten in terms of this re-defined $\mathcal{H}_1(t)$, is

$$\frac{d\rho}{dt} = -i\left[(\mathcal{H}_0 + \overline{\mathcal{H}_1}) + \mathcal{H}_1'(t),\ \rho\right], \tag{29}$$

which can be converted into an expression analogous to Eq. (27) after ρ and $\mathcal{H}_1'(t)$ are transformed into the interaction representation based on the new static Hamiltonian, i.e.,

$$\rho^* = \exp\left(i\,(\mathcal{H}_0 + \overline{\mathcal{H}_1})\,t\right) \cdot \rho \cdot \exp\left(-i\,(\mathcal{H}_0 + \overline{\mathcal{H}_1})\,t\right) \tag{30}$$

and

$$\mathcal{H}_1'^*(t) = \exp\left(i\,(\mathcal{H}_0 + \overline{\mathcal{H}_1})\,t\right) \cdot \mathcal{H}_1'(t) \cdot \exp\left(-i\,(\mathcal{H}_0 + \overline{\mathcal{H}_1})\,t\right). \tag{31}$$

Since different spins in the sample experience different values of $\overline{\mathcal{H}_1}$, the calculation must use a distribution of rotating frames corresponding to these different values of $\overline{\mathcal{H}_1}$. Whereas the usual relaxation problem is to find the width of a single resonance signal centered at frequency $\omega_0 = \mathcal{H}_0/\hbar$, this problem involves finding the widths of each resonance line over a distribution of frequencies $\omega' = (\mathcal{H}_0 + \overline{\mathcal{H}_1})/\hbar$. The resonance lineshape which is calculated in this way is thus the envelope of a distribution of

broadened resonance spikes.

The width of these individual resonance spikes may be investigated by means of the Waugh multi-pulse averaging sequence.[47, 48] This sequence essentially averages $\mathcal{H}_1$ to zero at a rate which is fast compared to the effective dipolar interaction. If, however, local motions are fast compared to the time scale of the pulse cycle, the resulting linewidth observed in the spectrum measures these local field fluctuations, which are not affected by this sequence.

A spectrum obtained[49] by performing this averaging sequence on a sample of unsonicated dimyrisotyl lecithin bilayers is shown in Fig. 7. The pulse cycle time was 60 μsec for an eight-pulse sequence and the instrumental resolution was $\sim$ 10 Hz. Since the intermolecular dipolar broadening can be estimated as $\sim$20 Hz or less[28] in this case, the observed methylene proton linewidth of $\sim$100 Hz measures essentially the residual intramolecular dipolar broadening. The correlation times corresponding to this width are $\tau_\perp \sim 10^{-7}$ sec and $\tau_\parallel$ any time shorter than this $\tau_\perp$. This method provides an independent test of the $\tau_\perp$ obtained from T_1 studies, and confirms the physical picture of the local motions of chains in unsonicated bilayers.

Effect of sonication. When bilayer sheets are subjected to prolonged ultrasonication they break up, forming in water a dispersion of small vesicles ($\sim$ 300 Å in diameter).[50] These vesicles tumble freely and therefore present a different motional

FIGURE 7

Waugh multi-pulse-narrowed lecithin pmr spectrum. This spectrum at 55 MHz of dimyristoyl lecithin bilayers was narrowed from an original width of ~ 3000 Hz by a Waugh multi-pulse sequence, with 60 μsec cycle time for a complete 8-pulse cycle and instrumental resolution ~ 10 Hz. The chemical shift reference has been corrected for the scaling effect of the pulse sequence. The choline methyl and chain methylene protons (2.1 ppm separation) can be distinguished.

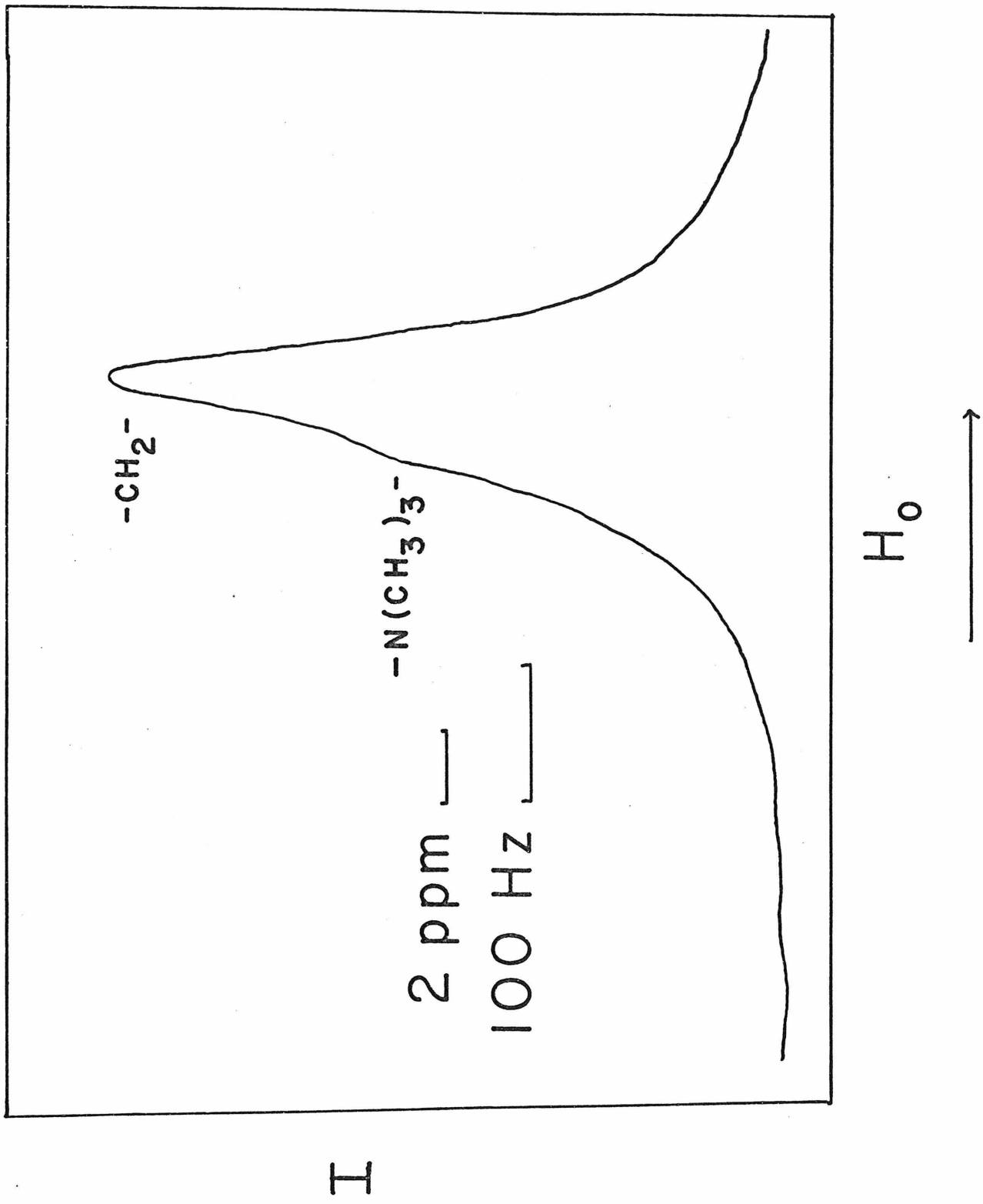
I
2 ppm
100 Hz
$-CH_2-$
$-N(CH_3)_3-$
H_o

narrowing problem from that encountered with bilayer sheets. Specifically, sonicated preparations of lipids show pmr signals which are only a few Hz in width. Furthermore, these signals show essentially 100% of the intensities expected, for all protons of the lipids.[51] Attempts have been made to account for this drastic narrowing of the resonance lines in terms of the effect of overall tumbling of the vesicles.[52] Other explanations hold that increased local motion due to irregularity of chain packing in the small vesicles produces the narrow lines.[53]

This question can be decided using Anderson theory, and involves only formulating a motional model for chain protons in these vesicles, deriving a form for $\omega(\tau)$, and evaluating T_2 by the method suggested in Eq. (5). The calculation will be performed for a pair of neighbor protons on a chain, since this will furnish a minimum intramolecular dipolar linewidth, and thus provide a lower limit to the degree of local motion present in sonicated vesicles.

The protons on lipid chains in sonicated bilayer vesicles have a complex overall motion which can be described with reference to Fig. 2. Let $\vec{r}$ in this figure be an interpair vector and $\vec{c}$ be the lipid chain axis vector. Then the motion has three parts: (i) motion of $\vec{c}$, because of overall vesicle tumbling, on a timescale τ_V, (ii) motion of $\vec{r}$ with respect to $\vec{c}$, causing changes in the angle β of $\vec{r}$ to $\vec{c}$, on a timescale $\tau_\perp$, and (iii) motion of $\vec{r}$ around $\vec{c}$, causing changes in the angle φ, on a timescale $\tau_\parallel$.

The angular part of the dipole-dipole interaction, in terms of the angles described in Fig. 2, may then be written as

$$\begin{aligned} 3\cos^2\theta - 1 &= \tfrac{1}{2}(3\cos^2\theta' - 1)\cdot(3\cos^2\beta - 1) \\ &+ 3\sin\theta'\cos\theta'\sin\beta\cos\beta\sin\varphi \\ &+ \frac{3}{2}\sin^2\theta'\sin^2\beta\cos 2\varphi \end{aligned} \tag{32}$$

Now the linewidth problem will reduce to calculating the average time fluctuations of this $(3\cos^2\theta - 1)$, given a model of vesicle tumbling for fluctuations in θ', and a model of local motion for fluctuations in β and φ.

It will be helpful to demonstrate an exact T_2 calculation for the case in which only one random function of time need be considered, instead of several as is the case in Eq. (32). For isotropic motion of a pair of spins, the free induction decay g(t) may be written as

$$\begin{aligned} g(t) &= \overline{\cos\left[\int_0^t \alpha(3\cos^2\theta(\tau) - 1)\,d\tau\right]} \\ &= \overline{\cos\left[\alpha\cdot\int_0^t \sqrt{\tfrac{4}{5}}\,p(\tau)\,d\tau\right]} \end{aligned} \tag{33}$$

where $p(\tau)$ is a random function such that $\overline{p} = 0$ and $\overline{p^2} = 1$. For times long compared to the timescale τ_c of the isotropic motion, the integral in Eq. (33) becomes

$$\alpha\int_0^t \sqrt{\tfrac{4}{5}}\,p(\tau)\,d\tau = \alpha\sqrt{\tfrac{4}{5}}\,\sqrt{t\cdot\tau_c} \tag{34}$$

The value

$$1/T_2 = \tfrac{4}{5}\,\alpha^2\,\tau_c$$

is then obtained by setting the right hand side of Eq. (34) equal to 1, the procedure mentioned earlier (Eq. 5). This T_2 is identical to that of Kubo and Tomita[22] for the conditions of interest here ($T_1 \gg T_2$).

This procedure is the basis of the T_2 calculation, and is modified only by the need for dealing with the several random functions $\theta'(\tau)$, $\beta(\tau)$, and $\varphi(\tau)$ on the right hand side of Eq. (32). Evaluation of $\int_0^t (3\cos^2\theta(\tau) - 1)\,d\tau$, as given in Eq. (32), requires two results on random functions. First, any random function a(t) may be represented in the form

$$a(t) = \bar{a} + \left\{ \overline{[a(t) - \bar{a}]^2} \right\}^{\frac{1}{2}} \cdot p(t) \qquad (35)$$

where $\overline{(a(t) - \bar{a})^2}$ is now just a constant (i.e., some average value, as denoted by the bar), and p is a new function of the type used in Eq. (33), such that $\bar{p} = 0$ and $\overline{p^2} = 1$. Second, the product of two random functions p_1 and p_2 of this type is a new function q, where $\bar{q} = 0$ and $\overline{q^2} = 1$, that has an effective correlation time τ_q such that

$$\frac{1}{\tau_q} = \frac{1}{\tau_{p_1}} + \frac{1}{\tau_{p_2}} \qquad (36)$$

This expression is correct when p_1 and p_2 are uncorrelated, as will be the case for vesicle tumbling and local motion. An

immediate consequence of this result is that the effective correlation times of the second and third terms on the right hand side of Eq. (32) are of the order of $\tau_{\|}$, which is the fastest correlation time in the model. These terms can be neglected in comparison with the first, as their inclusion would lead only to a slightly greater linewidth. With this simplification, and results (35) and (36), the form of $\int_0^t \omega(\tau)\, d\tau$ becomes

$$\int_0^t \omega(\tau)\, d\tau = \frac{\alpha}{2}\sqrt{\tfrac{4}{5}}\left\{\bar{d}\cdot\sqrt{t\cdot\tau_v} + \overline{(d'^2)}^{\frac{1}{2}}\sqrt{t\cdot\tau_*}\right\} \qquad (37)$$

The expression for T_2 is derived as usual by setting Eq. (37) equal to 1, giving the result

$$\frac{1}{T_2} = \frac{1}{5}\alpha^2\left\{\bar{d}^2\cdot\tau_v + 2\bar{d}\,\overline{(d'^2)}^{\frac{1}{2}}\cdot\sqrt{\tau_v\cdot\tau_*} + \overline{d'^2}\cdot\tau_*\right\} \qquad (38)$$

where

$$\frac{1}{\tau_*} = \frac{1}{\tau_v} + \frac{1}{\tau_\perp},\quad \bar{d} = \overline{(1 - 3\cos^2\beta)},\ \text{and}\ d'^2 = \overline{\left[\bar{d} - (1 - 3\cos^2\beta)\right]^2}$$

Since τ_v, $\tau_\perp$ and $\Delta\beta$ are known for a given motional model, this expression gives us a minimum dipolar intramolecular linewidth under the conditions $\tau_v < 1/(\alpha\,\bar{d})$ and $\tau_\perp < \tau_v$.

The resulting possible minimum linewidths for different motional states are shown in Fig. 8. The linewidth is plotted against values of $\tau_\perp$ for local motion, for different values of $\Delta\beta$ (50°, 60°, 70°) and two different vesicle tumbling times (10^{-5} sec, 10^{-6} sec). These values of $\Delta\beta$ include the range of

FIGURE 8

PMR linewidth of methylene protons in sonicated bilayers. The linewidth of a chain methylene proton in a sonicated bilayer vesicle is plotted against $\tau_\perp$, timescale of local flexing motion, for a range of values of $\Delta\beta$ (extent of flexing, as defined in text) and two values of τ_v, vesicle tumbling time. The most probable parameter values are $\tau_v \sim 5 \times 10^{-6}$ sec (250 Å diameter vesicles) and $\Delta\beta \sim 65°$, $\tau_\perp \sim 10^{-7}$ sec (typical local motion in unsonicated bilayers), predicting a linewidth of several hundred Hz. The dashed and dotted line (-· -) for $\Delta\beta = 90°$ is included for comparison. This line is calculated on the assumption $\tau_\perp < \tau_v$.

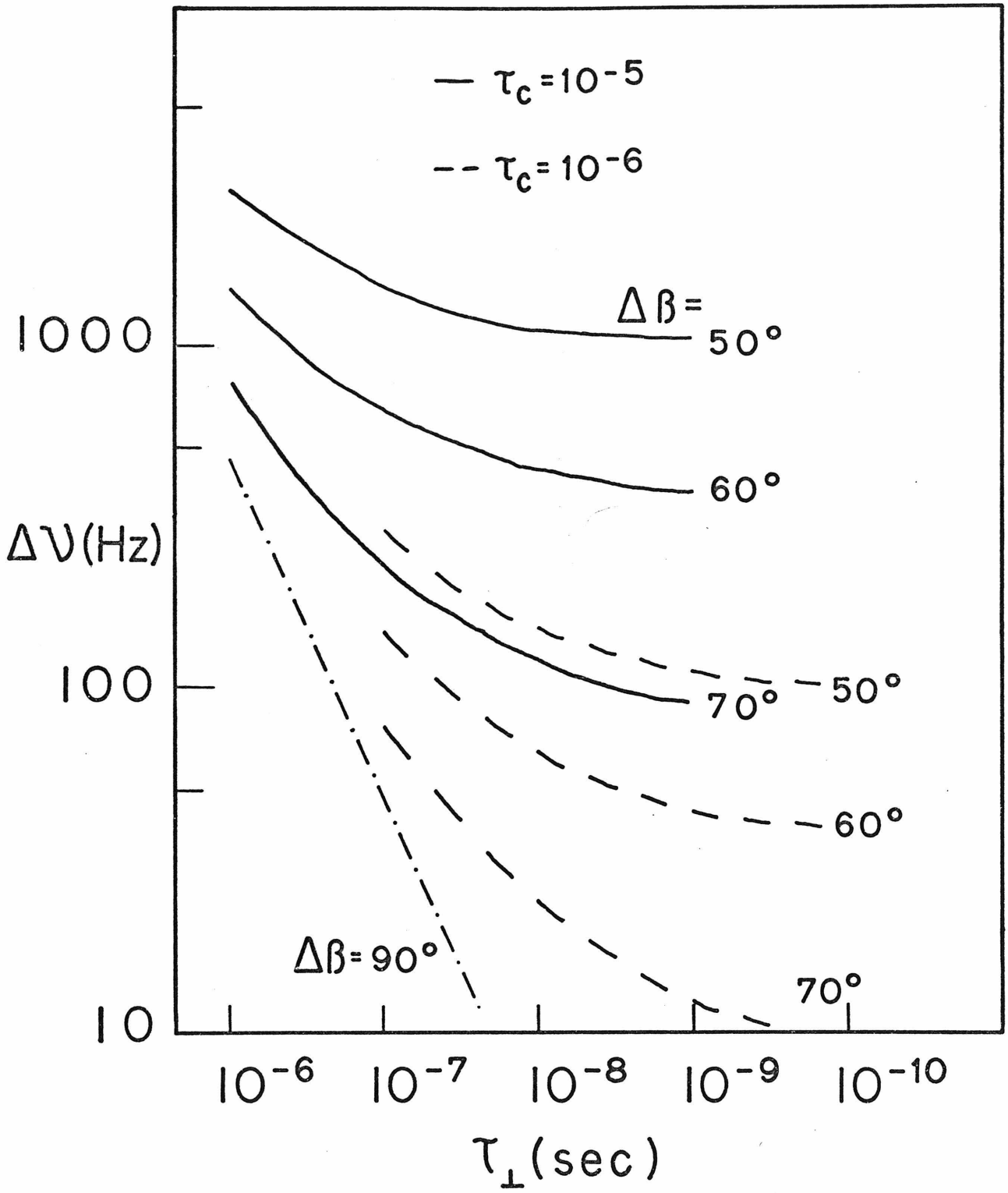
— $\tau_c = 10^{-5}$
-- $\tau_c = 10^{-6}$
$\Delta\beta =$
50°
60°
70°
50°
60°
70°
$\Delta\beta = 90°$
1000
100
10
$\Delta\nu$(Hz)
10^{-6}
10^{-7}
10^{-8}
10^{-9}
10^{-10}
$\tau_\perp$(sec)

likely values of this parameter for the local motion in unsonicated bilayers, and the values of τ_V are those possible for small (~250 Å diameter) vesicles. The most probable values of all these parameters ($\tau_V \sim 5 \times 10^{-6}$, $\tau_\perp \sim 1 \times 10^{-7}$, $\Delta\beta \sim 60°$) give a linewidth of several hundred Hz for typical chain protons. Therefore, simple superposition of overall vesicle tumbling on the local motions of chains in bilayers is not enough to explain the linewidth observed for the chain protons in vesicles. Additional local motion of the lipid chains in vesicles is therefore implied by these linewidth results. With the help of Eq. (38), a quantitative estimate of this additional motional freedom may be obtained.

The true pmr linewidth of methylene protons in vesicles, corrected for chemical shift spread of the methylene region, is approximately 5 Hz.[51] This implies that the sum of the three terms on the right side of Eq. (38) is 15 sec^{-1} or less. Given $\tau_V \sim 5 \times 10^{-6}$ sec, a representative vesicle tumbling time, this in turn implies values of $\Delta\beta$ greater than 80° and values of $\tau_\perp$ faster than 5×10^{-9}. The amplitudes of local motion are thus significantly larger in sonicated vesicles than in unsonicated bilayers, and the timescale of this motion is roughly 100 times faster.

An immediate consequence of this increased local motion is that the first and second terms on the right in Eq. (38) become small compared to the third term. Under these conditions the rate of overall vesicle tumbling will not be an important

determinant of the linewidth. Thus changes in solution viscosity, which produce changes in τ_v, should have little effect on observed linewidths, and this is found experimentally.[53] As $\Delta\beta \rightarrow 90°$, all motional narrowing is accomplished by the local motion, given $\tau_\perp < \tau_v$, and the effects of tumbling rate are negligible.

Previous treatments of pmr linewidths arising from vesicles have met with several difficulties,[52] briefly for lack of a systematic way of dealing with terms other than the first in Eq. (38). When the local motion is infinitely fast ($\tau_\perp \rightarrow 0$), as these investigators have correctly noted, the linewidth expression takes the form

$$1/T_2 \sim |\alpha\bar{d}|^2 \cdot \tau_v \qquad (39)$$

The effective reduced linewidth $\alpha\bar{d}$ has replaced the usual rigid lattice dipolar width α.[54] In the analogous narrowing problem of "magic angle" sample rotation superimposed on local motion, a similar result is found when the local motion is infinitely fast.

The physical situation, however, for lipid bilayers is that the relevant timescale, $\tau_\perp$, of local motion is not sufficiently fast compared to typical τ_v values that the approximation (39) above may be used. If a bilayer section could be tumbled at $\tau_v = 5 \times 10^{-6}$ sec with no perturbation of its local structure, the third term in Eq. (38) would dominate the expression and give a pmr linewidth for chain protons of several hundred Hz. The effect of a rapid $\tau_\parallel$ has been accounted for by dropping two possible broadening terms in Eq. (32), and it is important to note the different effects

of the $\tau_\perp$ and $\tau_\parallel$ motions, a distinction which is not always appreciated.

Just as the third term in Eq. (38) represents a broadening contribution which is not removed by vesicle tumbling, a term $1/T^\dagger$ appears in the exact treatment of the narrowing effects of the Waugh multi-pulse sequence,[48] and this broadening contribution is not removed by the pulse sequence. Thus in both coherent (pulse or sample rotation) averaging methods and statistical (Brownian motion) averaging, expressions like Eq. (39) will generally not be adequate for calculating the linewidth effects of complicated motions.

The pmr linewidths observed from vesicles imply a looser chain packing of the lipids in sonicated bilayers than in unsonicated bilayers. The local motion of chains in vesicles is practically unrestricted and fast ($\tau_\perp < 5 \times 10^{-9}$ sec), and it is the rate of this local motion which controls the linewidth. This should be contrasted with the situation in unsonicated bilayers, in which chain motion is seriously restricted and slow ($\tau_\perp \sim 10^{-7}$ sec). In terms of the motional model presented earlier, the local motion of chains in vesicles consists of trans-gauche rotations, a mode usually associated with hydrocarbon liquids. This conclusion is compatible with other experimental results on vesicles, most notably measurements of the T_1's of methylene chain ^{13}C nuclei.[55] The lipid chains in sonicated and unsonicated bilayer samples are thus characterized by quite different motional states.

Summary

Two main conclusions about the physical state of the interior of lipid bilayers emerge from these nmr linewidth results. First, the chief mode of motion of the hydrocarbon chains in unsonicated lipid bilayers is "kink" formation or the related gauche$^+$ gauche$^-$ rotation-pair motions. This process occurs at a faster rate in bilayers than in true solids, but as a mode of motion it is nonetheless distinct from the type of chain motions present in hydrocarbon liquids. The lipid chains of sonicated bilayers, on the other hand, have much greater freedom, and the motional state of these chains very nearly resembles a liquid state.

This paper also demonstrates that the stochastic linewidth theory of P. W. Anderson[19] offers the most straightforward way of calculating nmr linewidths of spin species undergoing restricted motions, and can be readily extended to treat restricted local motions combined with overall Brownian tumbling. Even relatively complex spectra, such as those of methyl groups, may be conveniently simulated for all types of restricted motions. Biological investigations using nmr, for example, studies on tissues, nerves, membranes, or very large molecules, frequently demand an understanding of the effects of restricted motion on nmr linewidths, and calculations of the type performed here may be necessary.

REFERENCES

1. M. de Broglie and E. Friedel, Comp. Rend., 176, 738 (1923).
2. V. Luzzati and F. Husson, J. Cell Biol., 12, 207 (1962).
3. H. Davson and J. F. Danielli, "Natural Membranes," University Press, 1952.
4. J. D. Robertson, Progr. Biophys. Chem., 10, 343 (1960).
5. J. M. Steim, M. E. Tourtellotte, J. C. Reinert, R. N. McElhaney and R. L. Rader, Biochemistry, 63, 104 (1969).
6. M. H. F. Wilkins, A. E. Blaurock and D. M. Engelman, Nature, New Biol., 230, 72 (1971).
7. Y. K. Levine and M. H. F. Wilkins, Nature, New Biol., 230, 69 (1971).
8. A. G. Lee, N. J. M. Birdsall and J. C. Metcalfe, Biochemistry, 12, 1650 (1973).
9. W. L. Hubbell and H. M. McConnell, Proc. Nat. Acad. Sci., 63, 16 (1969).
10. W. L. Hubbell and H. M. McConnell, Proc. Nat. Acad. Sci. 64, 20 (1969).
11. S. I. Chan, G. W. Feigenson and C. H. A. Seiter, Nature, 231, 110 (1971).
12. J. Charvolin and P. Rigny, J. Magn. Resonance, 4, 40 (1971).
13. J. Charvolin and P. Rigny, Nature, New Biol., 237, 127 (1972).
14. G. J. T. Tiddy, Nature, 230, 136 (1971).
15. J. J. De Vries and H. J. C. Berendsen, Nature, 221, 1139 (1969).
16. K. D. Lawson and T. J. Flautt, Mol. Cryst., 1, 241 (1966).

17. Z. Veksli, N. J. Salsbury and D. Chapman, Biochim. Biophys. Acta, 183, 434 (1969).

18. E. G. Finer, A. G. Flook and H. Hauser, Biochim. Biophys. Acta, 260, 59 (1972).

19. P. W. Anderson, J. Phys. Soc. Japan, 9, 316 (1954).

20. M. Saunders and C. S. Johnson, Jr., J. Chem. Phys., 48, 534 (1968).

21. C. H. A. Seiter, G. W. Feigenson, S. I. Chan and M. C. Hsu, J. Amer. Chem. Soc., 94, 2535 (1972).

22. R. Kubo and K. Tomita, J. Phys. Soc. Japan, 9, 888 (1954).

23. G. E. Pake, J. Chem. Phys., 16, 327 (1948).

24. M. Fixman, J. Chem. Phys., 47, 2808 (1967).

25. H. M. McIntyre, T. B. Cobb and C. S. Johnson, Jr., Chem. Phys. Letters, 4, 585 (1970).

26. H. S. Gutowsky and G. E. Pake, J. Chem. Phys., 18, 162 (1950).

27. E. R. Andrew, J. Chem. Phys., 18, 607 (1950).

28. G. J. Kruger, Z. Naturforschung, 24A, 560 (1969).

29. P. Devaux and H. M. McConnell, J. Amer. Chem. Soc., 94, 4475 (1972).

30. E. R. Andrew and R. Bersohn, J. Chem. Phys., 18, 159 (1950).

31. T. B. Cobb and C. S. Johnson, Jr., J. Chem. Phys., 52, 6224 (1970).

32. W. L. Hubbell and H. M. McConnell, J. Amer. Chem. Soc., 93, 314 (1971).

33. M. Shporer and M. Civan, Biophys. J., 12, 114 (1972).

34. M. Civan and M. Shporer, Biophys. J., 12, 404 (1972).

35. P. J. Flory, "Statistical Mechanics of Chain Molecules", Interscience, New York, p. 60, 1969.

36. K. van Putte, J. Magn. Resonance, 2, 216(1970).

37. H. Traüble, J. Membrane Biol., 4, 193 (1971).

38. N. Pechhold, S. Blasenbrey and S. Woerner, Z. Kolloid., 189, 14 (1963).

39. A. Abragam, "The Principles of Nuclear Magnetism", Oxford University Press, London, Chapter 5, 1961.

40. D. E. Woessner, J. Chem. Phys., 36, 1 (1962).

41. P. S. Hubbard, Phys. Rev., 109, 1153 (1958).

42. V. J. McBrierty and D. C. Douglass, J. Magn. Resonance, 2, 353 (1970).

43. V. J. McBrierty, D. W. McCall, D. C. Douglass and D. R. Falcone, J. Chem. Phys., 52, 512 (1970).

44. G. W. Feigenson and S. I. Chan, J. Amer. Chem. Soc., in press.

45. S.I. Chan, C. H. A. Seiter and G. W. Feigenson, Biochem. Biophys. Res. Commun., 46, 1488 (1972).

46. See Ref. 39, p. 276.

47. U. Haeberlen and J. S. Waugh, Phys. Rev., 175, 453 (1968).

48. U. Haeberlen and J. S. Waugh, Phys. Rev., 185, 420 (1969).

49. R. W. Vaughan, C. H. A. Seiter, G. W. Feigenson and S. I. Chan, to be published.

50. C. Huang, Biochemistry, 8, 344 (1969).

51. S. A. Penkett, A. G. Flook and D. Chapman, Chem. Phys. Lipids, 2, 273 (1968).

52. E. G. Finer, A. G. Flook and H. Hauser, Biochim. Biophys. Acta, 260, 49 (1972).

53. M. P. Sheetz and S. I. Chan, Biochemistry, 11, 4573 (1972).

54. E. R. Andrew and A. Jasinski, J. Phys., C, 4, 391 (1971).

55. Y. K. Levine, N. J. M. Birdsall, A. G. Lee and J. C. Metcalfe, Biochemistry, 11, 1416 (1972).

PART III

SELECTED IMPLICATIONS

The papers presented here have several implications for the use of nmr in model membrane studies, and for the expected value of sonicated vesicles as a model membrane system. A few remarks are perhaps appropriate here about the more direct questions raised in each topic by this work.

The first relaxation lesson learned in both papers is that it is generally not profitable to try to use high-resolution nmr principles in analyzing spectra of systems characterized by severely restricted local motions. It is usually better to start with the rigid lattice powder spectrum for the spin species in question and introduce averaging effects into this spectrum, rather than to start with the high-resolution nmr spectrum of the system and introduce dipolar effects. Even such a simple system as the methyl rotor is found to have features of interest in its powder spectrum, and these features will be significant in the interpretation of many biological spectra. As was mentioned in the second paper, a similar situation also exists in magnetic resonance of quadrupolar nuclei, where restricted molecular motion leaves large splittings in the spectrum which will be missed on ordinary high-resolution nmr spectrometers. As more investigators perform studies of selectively deuterated bilayers, this phenomenon will become an increasingly serious pitfall in bilayer nmr.

The second relaxation lesson learned here is that simple intuitive linewidth theories have been very misleading in applications to complex molecular motions. For the slow motions characteristic of many aggregated biological systems, the direct computer simulation of linewidths using stochastic linewidth is feasible precisely because these motions are slow and require only short computer runs to simulate a free induction decay. The analytical theory presented here for the linewidth of protons in sonicated vesicles is correct for vesicle tumbling times of 10^{-5} sec or faster, and affords some insight into the details of motional narrowing in these systems, but for large vesicles tumbling at times slower than 10^{-5} seconds a direct simulation may be necessary, especially in the range 10^{-4}-10^{-5} seconds which may be of great practical interest.

Perhaps the most important applied result obtained here is the demonstration that chain packing in bilayers is seriously disturbed upon sonication, that is, the more pronounced the curvature of the bilayer surface the more disordered the arrangement of lipids. This conclusion, established by theoretical linewidth reasoning, has been supported by three experimental studies. First, Sheetz and Chan (Ref. 31 of Introduction) showed that changing the viscosity of a vesicle solution by a factor of ~ 30 by addition of DNA produced negligible linewidth changes in the lipid proton resonances. More recently, C. H. A. Seiter and D. Lichtenberg showed (unpublished results) that lipid vesicles

below the crystalline ⇌ liquid crystalline lipid phase transition temperatures have a methylene proton linewidth of ~ 800 Hz, indicating that the lipids in vesicles cannot be packed in the orderly fashion of lipids in multilayers below their transition temperature. Furthermore, P. A. Kroon and D. Lichtenberg (unpublished results) have changed the viscosity of vesicle solutions simply by changing the vesicle concentration, and observe no linewidth change from lipid protons over a tenfold change in solution viscosity. These observations provide extensive practical confirmation that proton linewidths from lipids in vesicles are controlled by rapid, nearly unrestricted local motion. As was pointed out in the second paper, these results demand changes in the physical picture of vesicles and multilayers presented by many earlier authors (Refs. 28, 30, 32, and 33), whose treatment of the problems of molecular motion was hampered by lack of a theory adequate for interpreting their linewidth observations.

The degree of order or disorder in a lipid bilayer is not purely a question of chemical physics but rather has an important bearing on the problems of protein binding and mobility in membranes and on permeability of bilayers to ions. E. Racker, for example, has speculated (Ref. 23 of Introduction) that the reason different lipids induce different efficiencies of oxidative phosphorylation in reconstituted mitochondrial vesicles is that different lipid mixtures produce different sizes of vesicles. It is quite easy to see how the curvature/packing situation in vesicles would affect

both the binding of the cytochromes and ATPase to these membranes and the permeability of the membranes to protons, a potentially crucial factor in oxidative phosphorylation.

The permeability of bilayers to a variety of substances should perhaps be studied as a function of vesicle size. Investigators have observed differences (Ref. 29 of Introduction) in the rate at which benzyl alcohol, for example, traverses sonicated bilayers, erythrocyte membranes, and macroscopic bilayer films. This type of investigation could make clear the relationship of bilayer curvature and lipid disorder to irreproducibilities in vesicle permeability studies, and might suggest the important physical characteristics of naturally occurring (e.g., synaptic) vesicle systems.

An application of this work which is more speculative in terms of biology but concrete in terms of nmr is the investigation of the mobility in bilayers of a large class of compounds which are involved in energy transduction and electron transport in bilayer membranes. Specifically, cis-11-retinal and vitamin A in optical membranes, vitamins Q and the K series in mitochondria, and carotene pigments and phytyl chains in chloroplasts all have as a common structural element variations on the repeating unit $(-CH_2-CH=\overset{CH_3}{\overset{|}{C}}-CH_2-)$. Just as a spin label perturbs the local packing of aliphatic chains in a bilayer, inducing increased mobility of the labelled as compared to unlabelled lipids, so the projecting methyl groups on these chains may serve a useful function by

perturbing the local chain structure and thus speeding the transport of these molecules through the bilayer. The methyl groups on these chains will be clearly observable by proton nmr even in unsonicated bilayer systems, allowing a variety of detailed mobility studies. This application is suggested as evidence that there is indeed much possible use still for proton nmr, and that perhaps the methyl groups naturally occurring in biological molecules may prove in many cases to be a sensitive probe of molecular motion.

PROPOSITION I

Coenzyme Q[1] has long been known to be a constituent of almost every type of cell; its discoverers in fact first called it ubiquinone because it appears everywhere. The form most common in mammalian cells, called CoQ_{10} (Fig. 1a) consists of a substituted quinone with a long attached isoprenoid chain. This molecule has been implicated in electron transfer in mitochondria,[2] and its semiquinone form is now believed[3] to shuttle electrons between mitochondrial flavoproteins and the cytochrome b/c_1 complex. The side chain in CoQ_{10} happens to be almost exactly the thickness of a lipid bilayer of the type found in mitochondria. It is proposed that the mobility of CoQ_{10} in phosphatidyl choline lipid bilayer vesicles be studied by nmr/epr methods, with a view to determining how fast CoQ_{10} could shuttle electrons between the inside and outside of a bilayer vesicle, and also how fast it can transport electrons laterally.

The methods for this study have already been established in two elegant papers[4, 5] by Kornberg and McConnell. They attached the spin label "TEMPO"[6] (Fig. 1b) to the choline head of the phosphatidyl choline molecule, the spin label replacing one of the choline methyl groups. This label molecule was then introduced into bilayer vesicles. The inside/outside transition rate of this molecule was measured by quenching the spin labels on the outside of the bilayers with sodium ascorbate, and watching the

recovery of the epr signal to a form similar to that observed originally, as spin labelled molecules from the inside layer of the vesicle diffuse to the outside. Lateral diffusion of the spin labelled molecules in the vesicles was measured by observing the line-broadening effect of the paramagnetic moiety of the spin label on theproton nmr resonance of choline group methyls at the bilayer surface. A knowledge of the effective distance dependence of this broadening effect allows a calculation of the rate of spatial diffusion of the phosphatidyl choline molecules.

The analogous experiments on CoQ_{10} incorporated into phosphatidyl choline bilayer vesicles may be carried out in two ways. First, the reduced form of CoQ_{10}[7] may be spin labelled using TEMPO-isothiocyanate (Fig. 1c) labels commercially[8] available, which attach to hydroxyl groups under mild conditions. There are two hydroxyls available to be labelled, but the one-label and two-label forms should be chromatographically separable, and only a small quantity (one labelled CoQ_{10} per 100 phosphatidyl cholines) is needed. With TEMPO-CoQ_{10} the Kornberg-McConnell experiments can be carried out exactly as for TEMPO-lecithin, and the Spin Label Kit also provides isothionate labels of different attaching chain lengths, so that the spin label's perturbation to molecular mobility may be estimated.

A biologically more direct but physically more demanding approach involves generating paramagnetic centers directly rather than attaching a spin label. The semiquinone form of CoQ_{10} has

been studied by epr in alkaline solution, [9] and quinones are known to be reasonably stable in alkaline solution from classical organic chemistry. Bilayer vesicles incorporating reduced CoQ_{10} could be made up in alkaline solution, and from the free radical concentration established by epr measurements, the lateral diffusion experiment could be carried out. The inside/outside diffusion experiment would probably be possible in this system only if the inside/outside diffusion rate for CoQ_{10} were fast compared to the proton diffusion rate across vesicles of pure phospholipid, since otherwise the effect of quenching the outside radicals by a proton pulse would lead to a changing "inside" signal which disappears as the protons leak through the bilayer. This experiment is interesting, however, because whether the TEMPO or semiquinone form is more simply performed, it would give some idea of the possible physical chemical function of CoQ_{10}'s long isoprenoid tail, a molecular form which occurs in many "transport" molecules.

123

Fig. 7

Co Q_{10} ox

a)

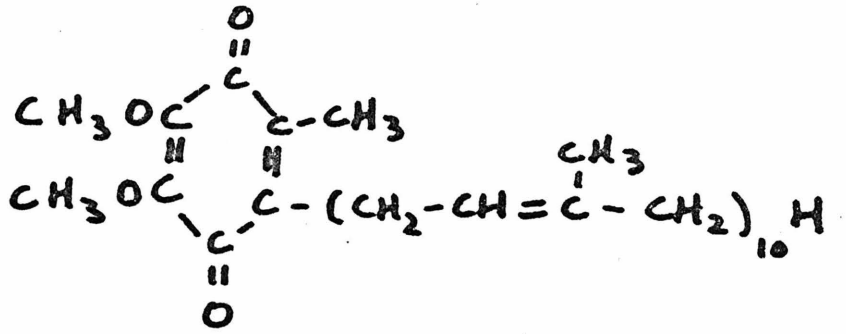

Co Q_{10} RED

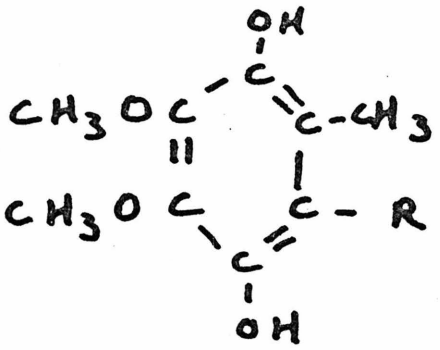

"TEMPO"

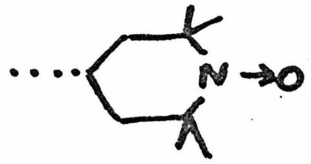

b

"TEMPO" ISOTHIOCYANATE

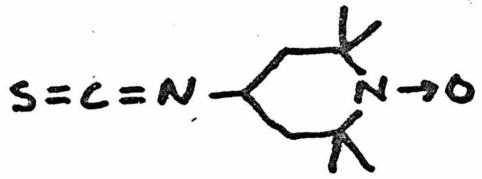

c

REFERENCES

1. G. E. W. Wolstenholme and C. M. O'Connor, eds., "Quinones in Electron Transport", Little, Brown and Co., Boston, 1960.
2. A. L. Lehninger, "Bioenergetics", W. A. Benjamin, Menlo Park, 1971.
3. D. Bäckström, B. Morling, A. Ehrenberg and L. Ernster, Biochim. Biophys. Acta, 197, 108 (1970).
4. R. D. Kornberg and H. M. McConnell, Biochemistry, 10, 1111 (1971).
5. R. D. Kornberg and H. M. McConnell, Proc. Nat. Acad. Sci., 68, 2564 (1971).
6. H. M. McConnell and B. G. McFarland, Quart. Rev. Biophys., 3, 1 (1970).
7. Calbiochem, La Jolla, California 92037. Cat. 661611.
8. Syva Associates, Palo Alto, California 94304. "Spin Label Kit E".
9. M. S. Blois, Jr. and J. E. Maling, Biochem. Biophys. Res. Commun., 3, 32 (1960).

PROPOSITION II

The application of multi-pulse nmr[1] to problems of biological interest has been hampered by three factors. First, the original equipment[2] used to develop the techniques was expensive and difficult to use. Second, the potential users of the technique have doubtless found the abstract formulation[3, 4] of magnetic resonance favored by multi-pulse investigators rather inaccessible. Third, the signal-to-noise problem in dilute biological systems places some demands on the instrumentation.

These problems have at present largely been overcome. Reasonably inexpensive spectrometers[5] offering excellent resolution have been designed, the explanation of multi-pulse theory to non-specialists has started, [6] and the S/N problem in many cases (^{13}C for example[7]) may be less damaging than in conventional nmr. The experiment proposed here takes advantage of this rapidly improving situation.

Cytochrome c, one of the most important electron transport proteins in the mitochondrial oxidative phosphorylation[8] scheme, binds to lipid bilayers in high concentrations[9] (one cytochrome per 42-50 lipid molecules[10]). This protein is ideal for studying the orientation of proteins in lipid bilayers, for several reasons. The high resolution X-ray[11] spectrum

of cytochrome c has been established and analyzed extensively. The high resolution nmr spectrum has been obtained[12] in solution and at physiological pH the spectrum of oxidized cytochrome c covers an enormous chemical shift range, [13] from 35 ppm downfield (porphyrin ring methyls) from DSS ((3-trimethyl silyl) propane sulfonic acid sodium salt) to 24 ppm upfield for one ligand methionine methyl, a range of 60 ppm in all. In the proposed experiment, the lipid bilayers to which the cytochrome is bound are oriented between glass cover slips, [14] and thus the absolute orientation of the cytochrome with respect to the bilayers may be investigated. The chief outlying peaks (porphyrin methyl and methionine methyl) are easily assignable in a multi-pulse spectrum by comparison of spectra of the oxidized and reduced cytochromes, [15] and the concentration of protein is possible in this system that signal to noise is sufficient for observation (approximately 10^{-2} M protein could be introduced in the sample, or approximately 3×10^{-2} M methyl protons). From rotation of the oriented bilayer package in the applied magnetic field, the orientation of these methyls and hence of the protein may be deduced. The protein motion could conceivably be fairly free, which would spoil features of this experiment but would constitute interesting information in its own right, and the multi-pulse experiment might be able to establish the timescale of this motion.

REFERENCES

1. J. S. Waugh, C. H. Wang, L. M. Huber and R. L. Vold, J. Chem. Phys., 48, 662 (1968).
2. J. D. Ellett, Jr., M. G. Gibby, U. Haeberlen, L. M. Huber, M. Mehring, A. Pines and J. S. Waugh, Adv. Mag. Res., 5, 117 (1971).
3. P. Mansfield, J. Phys., C, 4, 1444 (1971).
4. U. Haeberlen and J. S. Waugh, Phys. Rev., 185, 420 (1969).
5. R. W. Vaughan, D. D. Elleman, L. M. Stacey, W. K. Rhim and J. W. Lee, Rev. Sci. Instr., 43, 1356 (1972).
6. R. W. Vaughan, Ann. Rev. Mat. Sci., 4 (to appear) (1974).
7. A. Pines, M. G. Gibby and J. S. Waugh, J. Chem. Phys., 59, 569 (1973).
8. A. L. Lehninger, "The Mitochondrion", Benjamin, New York (1964).
9. D. Green and S. Fleischer, Biochim. Biophys. Acta, 70, 554 (1963).
10. K. M. Ivanetick, J. J. Henderson and L. S. Kominsky, Biochemistry, 12, 1822 (1973).
11. R. E. Dickerson, T. Takano, D. Eisenberg, O. B. Kallai, L. Samson, A. Cooper and E. Margoliash, J. Biol. Chem., 246, 1511 (1971).
12. R. K. Gupta and A. G. Redfield, Science, 169, 1204 (1970).
13. R. K. Gupta and S. H. Koenig, Biochem. Biophys. Res.

Commun., 45, 1134 (1971).

14. Y. K. Levine and M. H. F. Wilkins, Nature, New Biol., 230, 69 (1971).

15. C. C. McDonald and W. D. Phillips, Biochemistry, 12, 3170 (1973).

PROPOSITION III

Magnetic Resonance Studies of Ribonuclease Folding

A series of articles[1-3] by R. L. Baldwin and co-workers has suggested that the folding and unfolding reactions of bovine pancreatic ribonuclease proceed through a series of partially folded intermediate conformations. Their experiments observe the folding and unfolding kinetics of ribonuclease after fast pH jump and temperature jump perturbations are performed on the ribonuclease in solution. The kinetics of the subsequent folding reactions cannot be described by a simple two-state folded $\rightleftharpoons$ unfolded model of the protein's conformation, and therefore imply that several intermediate states lie on the unfolding reaction pathway.

The proposed experiment is an attempt to characterize these intermediate states using proton nuclear magnetic resonance (nmr). Ribonuclease has been the subject of several nmr studies[4-8] and certain regions of its spectrum are unambiguously assigned. Preliminary studies of ribonuclease unfolding in guanine hydrochloride[9, 10] have been reported, studies which present some evidence for intermediate states of unfolding from observation of the C2 proton resonances of the four RNase histidine residues.

This proposal, however, is rather different from these equilibrium folding studies, and aims at direct characterization

of the intermediate states by combining nmr methods with pH and temperature jump kinetic methods. This approach may be described in four steps.

1. All exchangeable protons of an RNase sample will be replaced with deuterium nuclei. Totally deuterated ribonuclease could perhaps be obtained but this is not necessary.

2. The protein is "jumped" for a very short time, to a pH at which unfolding can occur. The solution during this short time will be made to contain a supply of protons which can rapidly exchange with the protons of certain amino acids, preferentially of those amino acids on partially unfolded segments.

3. The protein is quickly jumped back to refolding conditions. Exchange of most RNase protons in the molecule's folded state takes hours and longer. Thus the protein has a record of the partially folded exchange conditions which are "frozen" into the molecule for a long time.

4. Proton nmr spectra of this special ribonuclease can then be taken on a superconducting magnet nmr spectrometer equipped with a Fourier transform accessory. The resultant spectrum should show the folding history of the protein.

There are several reasons for expecting success with this approach. First, the pH jump method allows selection of conditions under which exchange is very fast for some protons, e.g., phenolic or imidazole protons, and slow for others. This selectivity simplifies the resulting difference spectra. Second, the

superconducting magnet spectrometer (220 MHz or higher) to be used in these studies provides enough chemical shift separation to observe several different protons of interest. NMR studies at lower fields have often been hampered by the lack of resolution, especially in the region of the water signal in the spectrum.

The general goal of this type of study is the development of really predictive folding rules for proteins, i. e., given the amino acid sequence of a protein to predict the folwing pattern. Ribonuclease is especially suitable for this investigation because its totally folded structure is well understood. (11)

REFERENCES

1. T.Y. Tsong, R. L. Baldwin and E. L. Elson, Proc. Nat. Acad. Sci., 68, 2712 (1971).
2. T.Y. Tsong and R. L. Baldwin, J. Mol. Biol., 69, 149 (1972).
3. T. Y. Tsong, R. L. Baldwin, P. McPhir and E. L. Elson, J. Mol. Biol., 63, 453 (1972).
4. D. H. Meadows, J. L. Markley, J. S. Cohen and O. Jardetzky, Proc. Nat. Acad. Sci., 58, 1307 (1967).
5. D. H. Meadows, O. Jardetzky, R. M. Epand, H. H. Ruterjans and H. A. Scheraga, Proc. Nat. Acad. Sci., 60, 766 (1968).
6. C. C. McDonald and W. D. Phillips, J. Amer. Chem. Soc., 91, 1513 (1969).
7. F. W. Benz, J. Feeney and G. C. K. Roberts. J. Magn. Resonance, 8, 114 (1972).
8. D. G. Westmoreland and C. R. Matthews, Proc. Nat. Acad. Sci., 70, 914 (1973).
9. F. W. Benz and G. C. K. Roberts, FEBS Letters, 29, 263 (1973).
10. J. H. Bradbury and N. L. R. King, Nature, 223, 1154 (1969).
11. G. Kartha, J. Bello and D. Harker, Nature, 213, 862 (1967).

PROPOSITION IV

1. Chemical Potential and Microscopic Probabilities

The thermodynamic functions of a fluid are conveniently connected in the relation[1]

$$\frac{\mu^E}{kT} = \frac{E^E}{NkT} - \frac{S^E}{Nk} + \left(\frac{PV}{NkT} - 1\right) \tag{1}$$

where the symbols have their usual thermodynamic meanings and the superscript E denotes excess quantities (i.e., X^E = X (fluid) - X (ideal gas)). For a fluid of hard spheres, that is, a fluid whose particles have the interparticle potential $u(r) = 0$ for $r > a/2$; $u(r) = +\infty$, $r \leq a/2$; a the particle diameter, this relation is especially useful, because of the ease with which μ^E may be obtained.[2, 3] Defining P_0 as the probability of inserting another particle into the system, one obtains the result

$$\mu^E = -kT \ln P_0 \tag{2}$$

To obtain additional information one can also define the following probability functions:[4]

$$h(s) = \text{probability that the center of the nearest hard sphere is exactly distance s away from a randomly chosen point} \tag{3}$$

$$P_0(s) = 1 - \int_0^s h(s')\,ds' = \text{probability that the nearest center is at least distance s away from a}$$

random point (4)

$$G(s) = -\frac{1}{4\pi s^2 P} \frac{\partial \ln P_0(s)}{\partial s}$$, the so-called contact radial distribution function (5)

A knowledge of $P_0(s)$ for a sufficient range in s thus allows one to calculate G(a), to be used in the hard sphere equation of state

$$\frac{PV}{NkT} - 1 = \frac{2}{3} \pi a^3 N/V \, G(a) \tag{6}$$

Since $E^E = 0$ for a fluid of hard spheres, one can also obtain S^E by using this information in Eq. (1).

The methods of scaled particle theory[4, 5] have been used to evaluate G(s), and the resulting equation of state was found satisfactory. More recently, the functions h(s) and $P_0(s)$ have been obtained directly[6] in a molecular dynamics[7] experiment, that is, a computer simulation of the behavior of systems containing large numbers of particles. The investigation was motivated by the hope that S^E would thus be obtainable by measurements at a single density.

2. A Cell Model for $P_0(s)$

A cell model essentially describes one idealized "particle neighborhood" which then replaces the N actual neighborhoods of the molecular dynamics experiment. If one stopped all the

particles of the fluid and assigned them in some way to cells, one could draw up a statistical map of the cell showing probably position of the particle in the cell. What one wants, in a first approximation, is a technique for obtaining such a statistical map a priori. This amounts to replacing the dynamics experiment with a Monte Carlo[8] experiment. Various approximate treatments for this map have been proposed, notably uniform density, and density determined by different potential wells.[9, 10]

A different model for the map is provided by the model of a particle undergoing a random walk with reflecting barriers. This model has three attractive features. First, the analytic solution of the problem[11] is available. For example, in one dimension the probability density is given by

$$P_t(r) = (2\pi t)^{-\frac{1}{2}} \sum_{K=-\infty}^{K=+\infty} \left[\exp\left(-(2K\ell - r)^2/2t\right) + \exp\left(-(2K\ell + r)^2/2t\right)\right]$$

for barriers at 0 and ℓ, with $0 \leq r \leq \ell$. Second, the exact shape of the distribution depends on the time over which the random walk is considered to be taking place. This time, essentially the mean time for escape from the cell, can be estimated from existing collision rate and free path data.[12] In the limiting case $t = \infty$, i.e., escape is impossible, the model goes to the uniform density treatment which is known[7] to be reliable for hard sphere solids. Third, and most importantly, the degree of central tendency of the distribution seems to agree very well with that which can be

estimated from experimental h(s) curves.

A number of other features enhance the value of this model. For example, the model can first be tested using a routine which picks random points in the cell and tabulates h(s). If these results compare satisfactorily with the experimental data, one could then develop the analytic theory for this function and hence $P_0(s)$ and G(s). Furthermore, modifications of the theory (e. g., different assignments of the free volume of the cell, non-zero probability that the cell is vacant) could be examined with reference to direct measurements on a molecular dynamics fluid.

Thus it is proposed that this particular model for the motion of a particle in the unit cell of a hand sphere fluid be tested, and the functions h(s), $P_0(s)$, and G(s) tabulated and compared with experiment.

REFERENCES

1. T. H. Hill, "Statistical Mechanics", McGraw-Hill, New York, Chapter, 1956.
2. B. Widom, J. Chem. Phys., 39, 2808 (1963).
3. T. L. Jackson and L. S. Klein, Phys. Fluids, 7, 228 (1964).
4. H. Reiss, H. L. Frisch and J. L. Lebowitz, J. Chem. Phys., 31, 369 (1959).
5. D. M. Tully-Smith and H. Reiss, J. Chem. Phys., 53, 4015 (1970).
6. C. H. A. Seiter and B. J. Alder (unpublished results).
7. B. J. Alder and T. E. Wainwright, J. Chem. Phys., 33, 1442 (1960).
8. M. N. Rosenbluth and A. W. Rosenbluth, J. Chem. Phys., 22, 881 (1954).
9. J. A. Barker, "Lattice Theories of the Liquid State, Pergamon Press, London, 1963.
10. K. E. Gubbins, W. R. Smith, M. K. Tham and E. W. Tiepel, Mol. Phys., 22, 1089 (1972).
11. W. Feller, "Introduction to Probability Theory and its Applications, Vol. II, John Wiley and Sons, New York, Chapter 10, 1966.
12. T. Einwohner and B. J. Alder, J. Chem. Phys., 49, 1458 (1968).

PROPOSITION V

Molecular dynamics studies,[1] and, more recently, integral equation techniques,[2] have shown that g(i), the radial distribution function, is determined for most simple fluids by the repulsive part of the intermolecular potential. This suggests that the microscopic structure of the fluid can be accurately modeled by a hard sphere fluid, and that the effect of the attractive part of the potential u(r) may simply be accounted for with a van der Waals term -a/V for the interval excess energy E^E (here a is a constant characteristic of the fluid, V the volume, and E^E defined in Proposition IV). This idea has raised hopes[3-7] that a satisfactory equation of state for a real fluid, e.g., liquid argon, could be developed in the form

$$\frac{PV}{NkT} = \frac{-a}{RTV} + \left[\frac{PV}{NkT} \text{ <hard sphere system at same density>}\right]$$

This type of equation has been shown to be a great improvement on the van der Waals equation at high densities.

A different calculation, in the spirit of this earlier work, is proposed for the model fluid of Proposition IV. One can assume the same spatial distribution for the particle in a cell, and introduce a test particle, calculating

$$P_0 = \exp(\overline{u(r)}/kT)$$

where the bar denotes averaging over the positions of the central particle. When one performs this calculation for a great number of locations of the test particle, one can then take

$$\mu^E = - kT \ln < P_0 >$$

where $< >$ denotes averaging over the position of the test particle. By performing this calculation over a sufficient range of densities P, one can also obtain the pressure

$$p = \int_0^\rho \rho' \left(\frac{\partial \mu}{\partial \rho'}\right)_T d\rho'$$

In combination with E^E, this information then yields a value for S^E (by relation (1) of Proposition IV).

This calculation has two attractive features. First, comparison of P_0 with the value obtained for the usual hard sphere experiment shows the influence of the attractive potential in a more detailed waythan does a van der Waals equation of state. Second, the results obtained from the calculation can be compared directly to Henry's law and vapor pressure data. This is possibly a more sensitive way to detect errors in P_0 than the usual comparison to critical data performed on the final equation of state. This type of comparison was attempted for scaled particle theory, [8] but the introduction of attractive potentials was sufficiently difficult that the calculation of chemical potentials for realistic u(r) was not performed. It is hoped that this method would allow extension of this otherwise powerful technique.

REFERENCES

1. B. J. Alder and C. E. Hecht, J. Chem. Phys., 50, 2032 (1969).
2. D. Chander and J. D. Weeks, Phys. Rev. Letters, 25, 149 (1970).
3. H. C. Longuet-Higgins and B. Widom, Mol. Phys., 8, 549 (1965).
4. E. A. Guggenheim, Mol. Phys., 9, 43 (1965).
5. E. A. Guggenheim, Mol. Phys., 9, 200 (1965).
6. I. R. McDonald and K. Singer, Mol. Phys., 23, 29 (1972).
7. I. B. Schrodt and K. D. Luks, J. Chem. Phys., 57, 200 (1972).
8. H. Reiss, H. L. Frisch, E. Helfand and J. L. Lebowitz, J. Chem. Phys., 32, 119 (1960).